Teaching Old Waves New Tricks: The Quest For Acoustic Meta-Materials

Nicholas Xuanlai Fang

Department of Mechanical Engineering
Massachusetts Institute of Technology
email: nicfang@mit.edu

MITMECHE

http://web.mit.edu/nanophotonics

Acknowledgement

Students and Postdocs

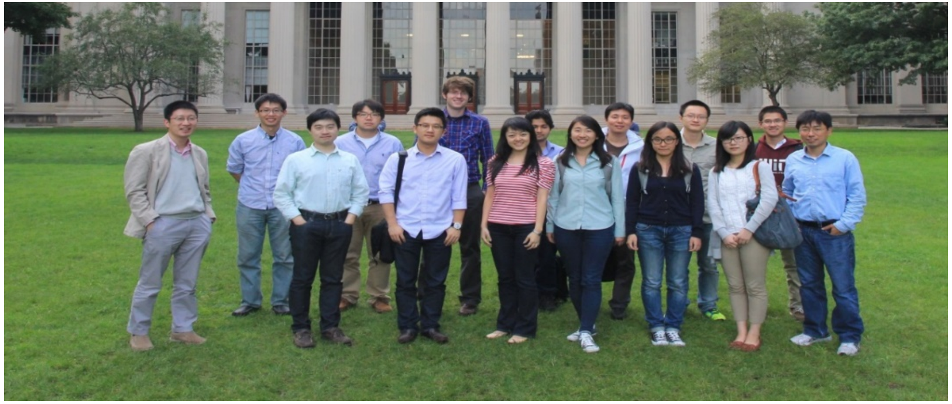

Support by:

- *ONR MURI*
- *DARPA*
- *AFOSR*
- *DTRA*
- *BASF*
- *NOAA Sea Grant*

Collaborators

Qiming Wang (USC)
Nicholas Boechler(UW)
Howon Lee (Rutgers)
Shengqiang Cai (UCSD)
Kevin Qi Ge, Martin Dunn (SUTD)
Keith Nelson and Alex Maznev(MIT)
Steve Johnson and Homer Reid(MIT)
Chris Spadaccini (LLNL)
Dan Tortorelli (UIUC)

Katia Bertoldi (Harvard)
Stephan Rudykh (Technion)
Pat Doyle, Linda Griffith, Paula Hammond (MIT)
Mary Boyce (MIT/Columbia)
Yun Jing (NCSU)
Tony Low, Phaedon Avouris (IBM)
Ned Thomas (Rice University)
Denis Lafarge (Univ Du Maine)

What Are Meta-Materials ?

Atomic Crystal Lattice

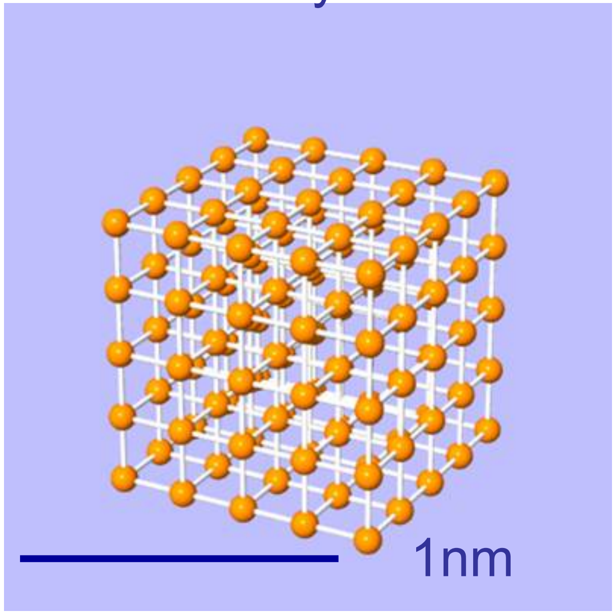

Sub-λ Meta “atoms”

Artificial nanostructures

(Yen, Fang et al Science 2004)

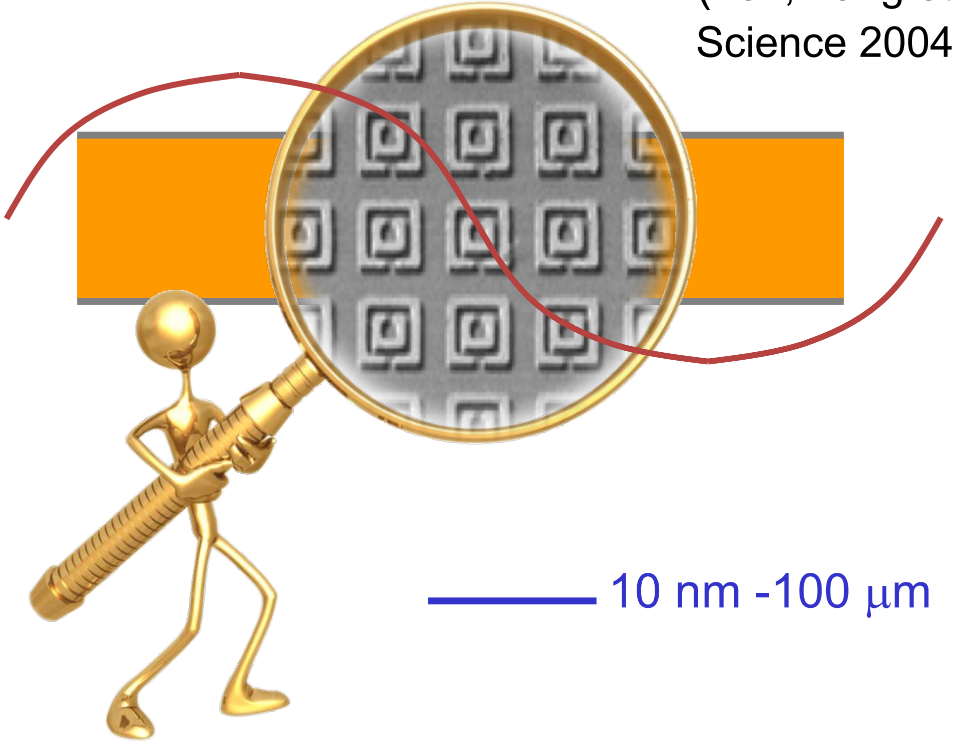

Exciting new physics!

- Optical magnetism
- Negative refraction
- super resolution imaging,
- wave shielding (cloaking)

e.g. Optical magnetism from split ring resonators

Research Vision and Missions

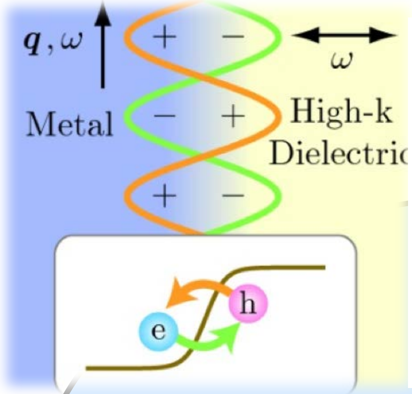

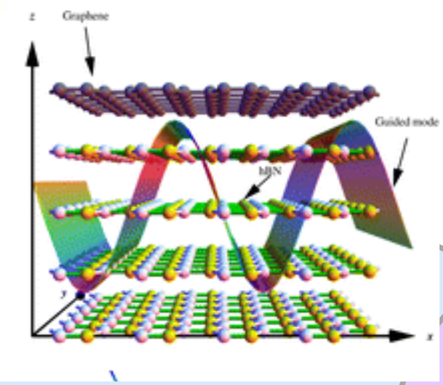

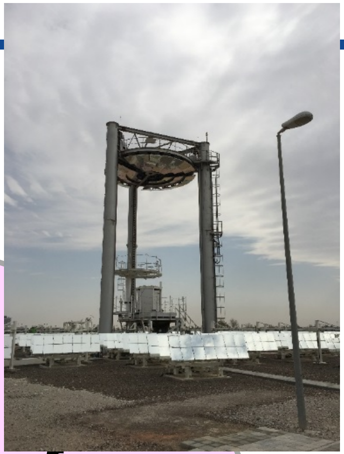

Fundamental study of Meta-materials

Application of Meta-materials

Micro/Nano Fabrication

Outline

- **Acoustic Meta-materials:**
  Quest for Thin Absorbers and Metalenses

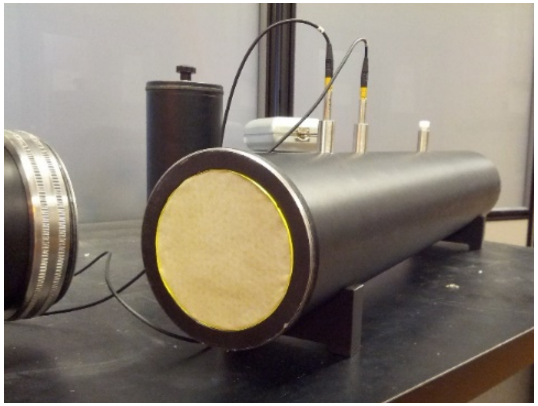

- **Micro/Nano Fabrication for Metamaterials**

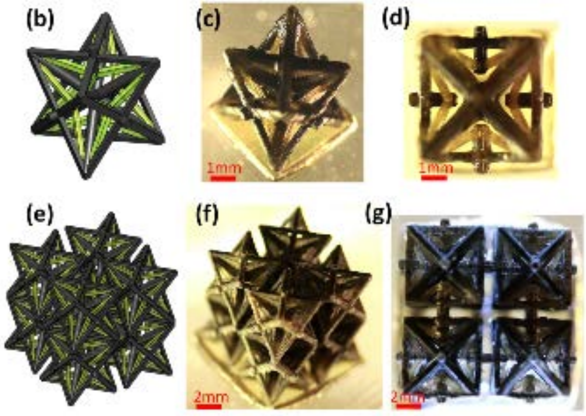

Why Manipulating Acoustic/Elastic Waves?

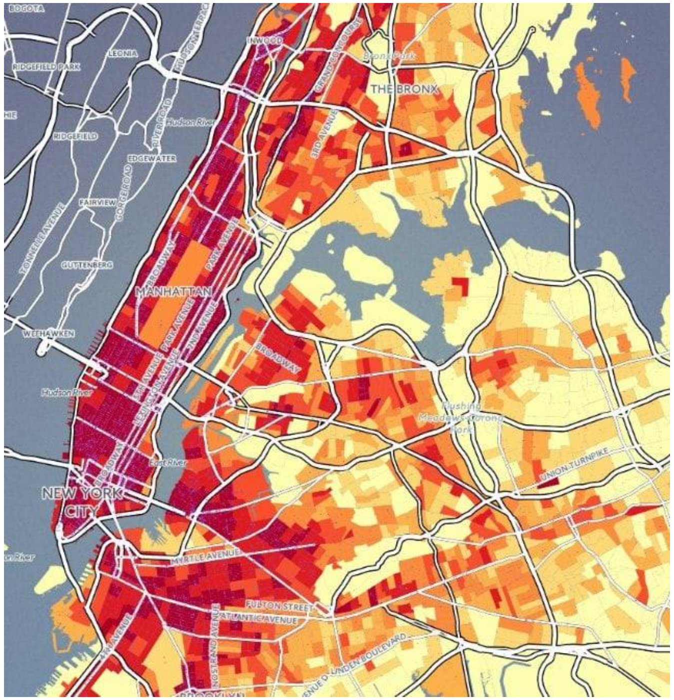

纽约噪音分布图

消音降噪

机房及数据中心

加工车间

医院病房

家用电器

Needs for Acoustic Materials Beyond Ashby Charts

Zhang et al, PRL 2011

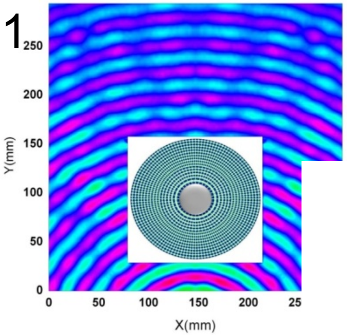

Anisotropy and inhomogeneity

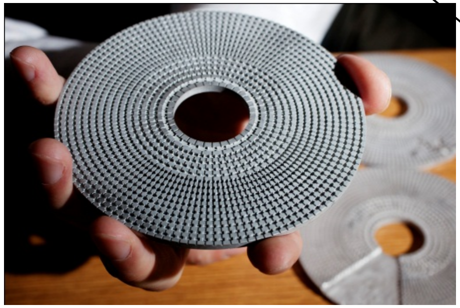

Zheng, Lee et al, Science 2014

Modulus

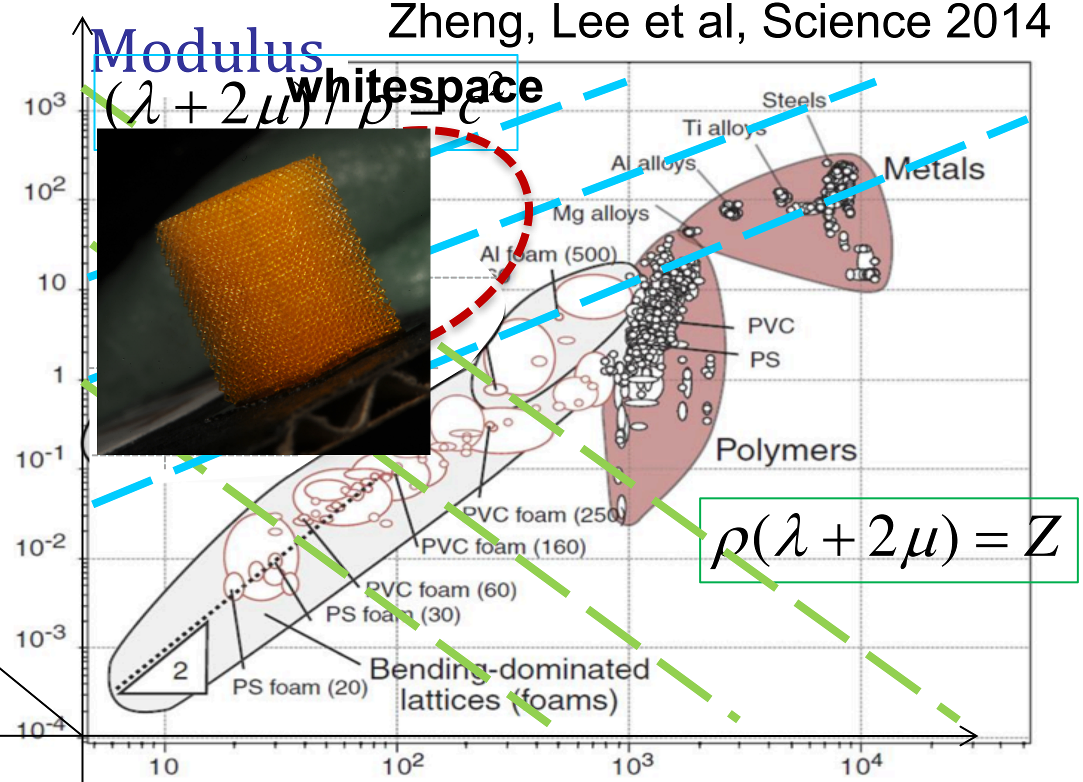

$$(\lambda+2\mu)/\rho=c^2$$

$$\rho(\lambda+2\mu)=Z$$

ρ: Density

Negative index medium ($\mu<0,\rho<0$)

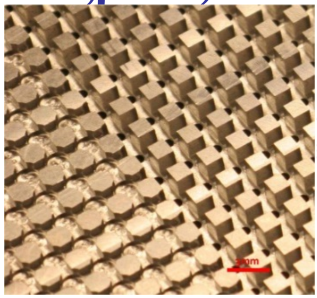

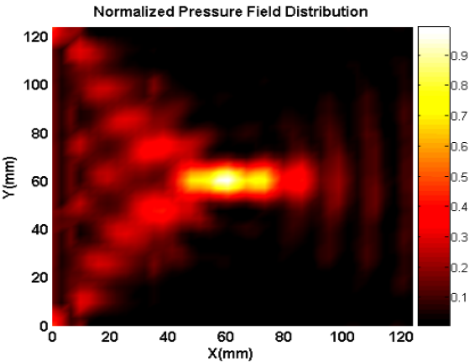

Zhang et al, PRL 2009

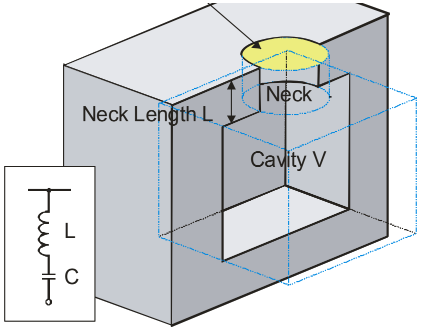

Fang et al, Nature Materials 2006

E.G. 交通轻量化需求新的环保隔音技术

Existing Materials

Synthetic Fabric

PET Felt

- 对于现代交通，安静出行是竞争的优势。全球汽车声学材料市场预计为100亿美元。
- 将钢铁和铝材料轻量化、把材料从钢换成树脂等，汽车，飞机和轨道交通系统轻量化的技术一直在发展，但是这样就会引起“引擎噪音变大”这一问题。
- 例如，福特在2015年轻量化概念车Mach II的研制报告中明确指出，减重的直接代价是车内隔振降噪性能的严重减弱。
- 由于空间的限制，发动机的低频噪音几乎无法阻挡。

> *“Car manufacturers nearly gave up blocking low frequency noise.”*
>
> *(Shuhei Nishimaki, Researcher at Nissan)*

为什么消除噪声是一个技术难题？

吸音和隔音屏障受到重量和体积限制，在低频率的性能表现欠佳

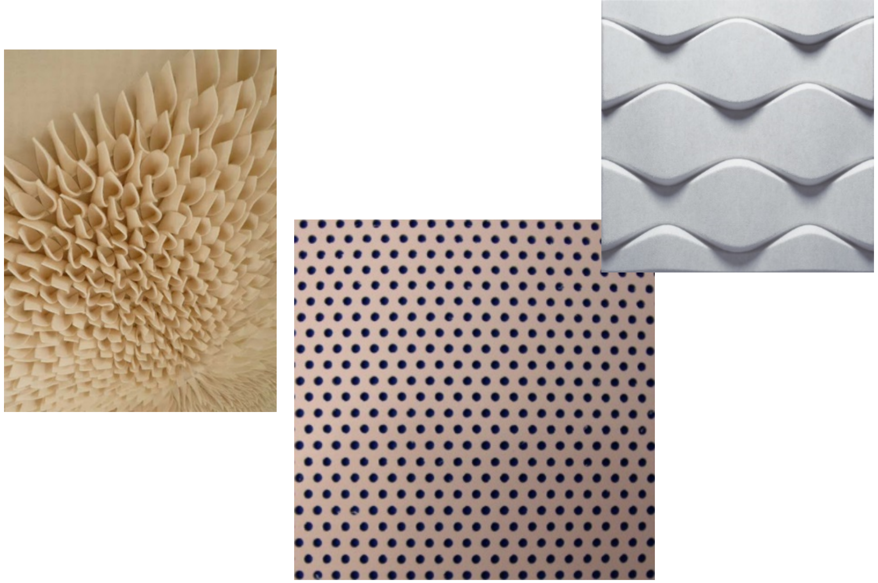

www.oxstyle.com

传统设计方法认为，声波通过有限厚度的阻隔材料的传输损耗，服从声质量法：

$$TL = 20log_{10}\left(\frac{P_i}{P_t}\right)$$
$$= 20log_{10}\left(\frac{t\pi\rho f}{\rho_0 c_0}\right)$$

t: *Thickness of infinite barrier*

ρ_0: *Density of air*

ρ: *Density of infinite barrier*

c_0: *Speed of sound in air*

f: *Frequency of sound*

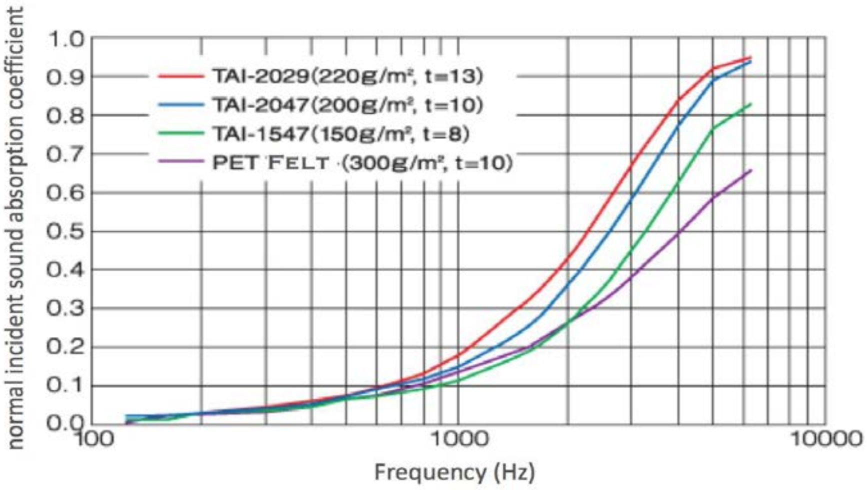

(source: design composite)

Overcoming Mass Law: Acoustic Meta Materials

- Acoustic Metamaterials, containing arrays of elastic resonators composed of a heavy core surrounded by a soft coating layer

- *Effective dynamic mass* of the system:

$$\rho_{eff} = \frac{Volume\ Averaged\ Stress}{Volume\ Averaged\ Acceleration}$$

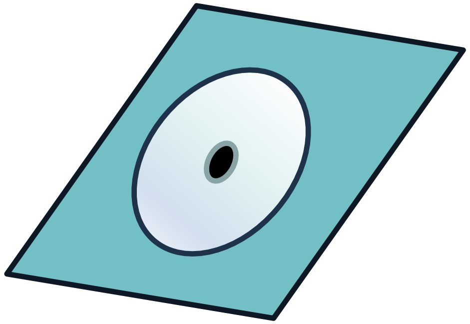

- ***Weak elastic moduli*** of the membrane results in low frequency oscillation patterns within a small and finite membrane with fixed boundaries.
- ***Near-total reflection*** can be achieved at a frequency between two vibrational eigenmodes where the in-plane average of displacement (normal to the membrane) is zero.

Simulation Results: Elastic Membrane

Typical Elastic Membrane

Membrane thickness: 0.25 mm
Elastic modulus: 7 MPa
Poisson’s ratio: 0.49

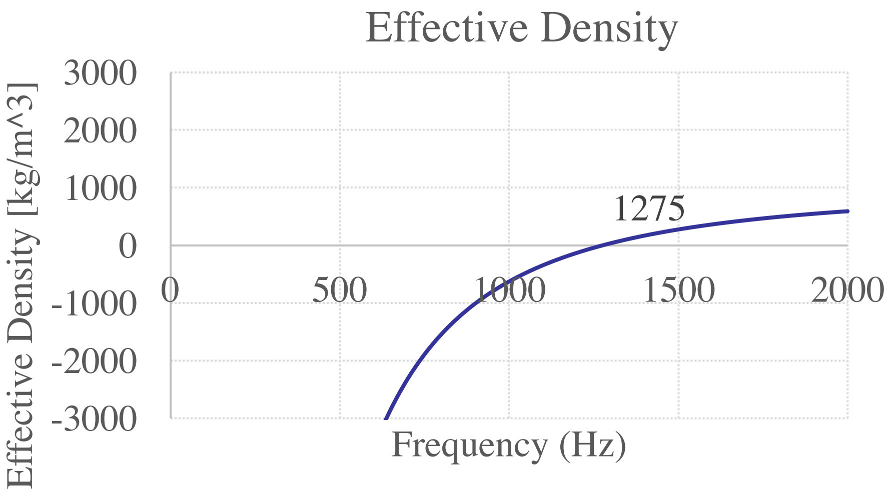
Effective Density

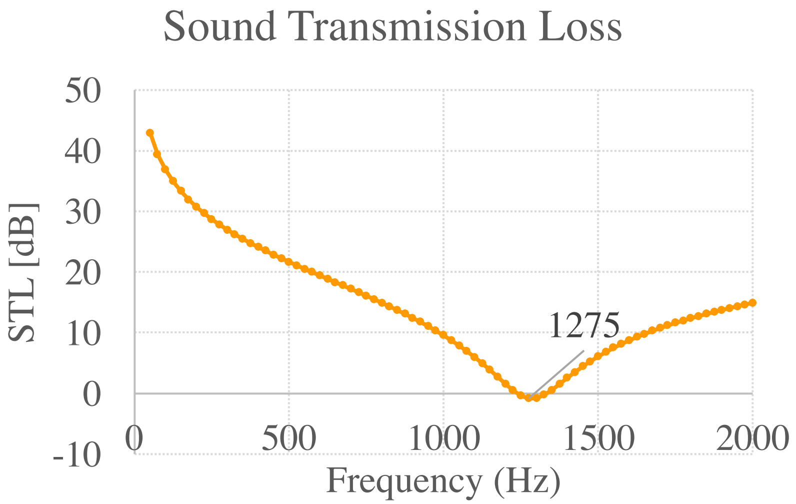
Sound Transmission Loss

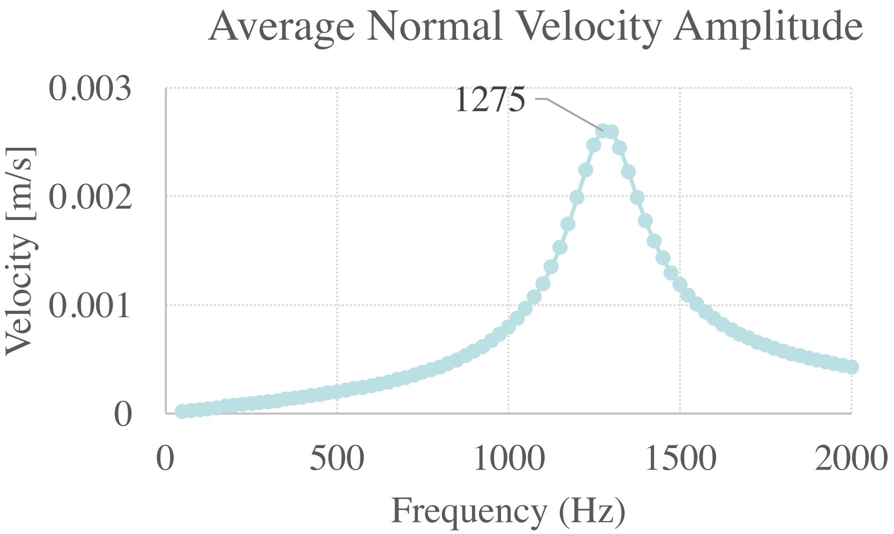
Average Normal Velocity Amplitude

Validation of Finite Element Simulation

Sound Transmission Loss

Membrane thickness: 0.20 mm natural rubber

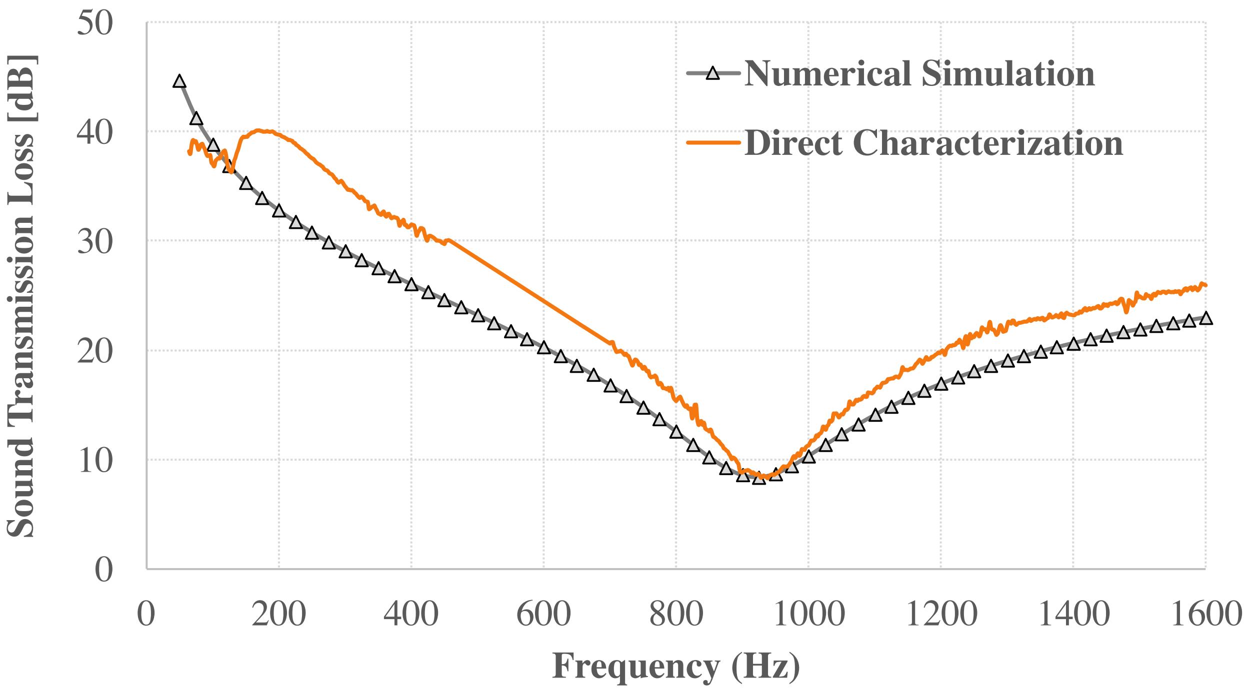

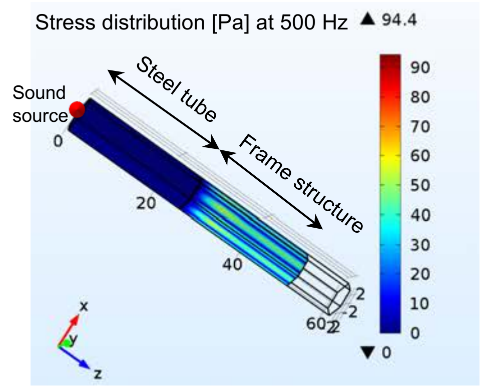

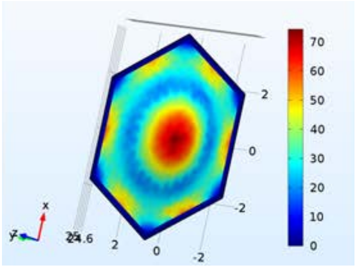

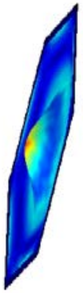

一种轻质隔音蜂窝薄膜材料

Dr Jun Xu

Dr Yun Jing (NCSU)

A lightweight yet sound-proof honeycomb acoustic metamaterial
Appl. Phys. Lett. **106**, 171905 (2015)

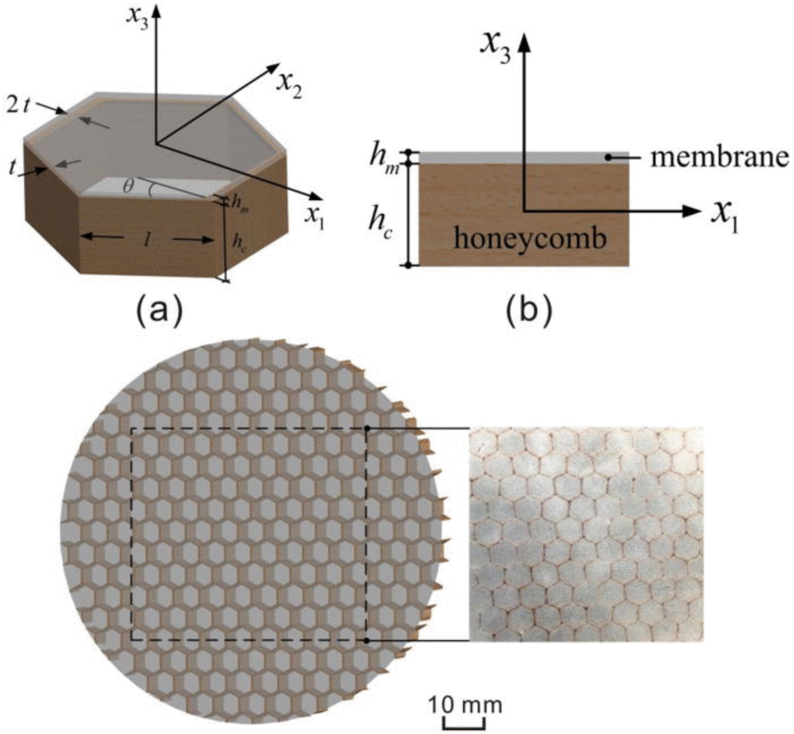

(a) (b)

(c)

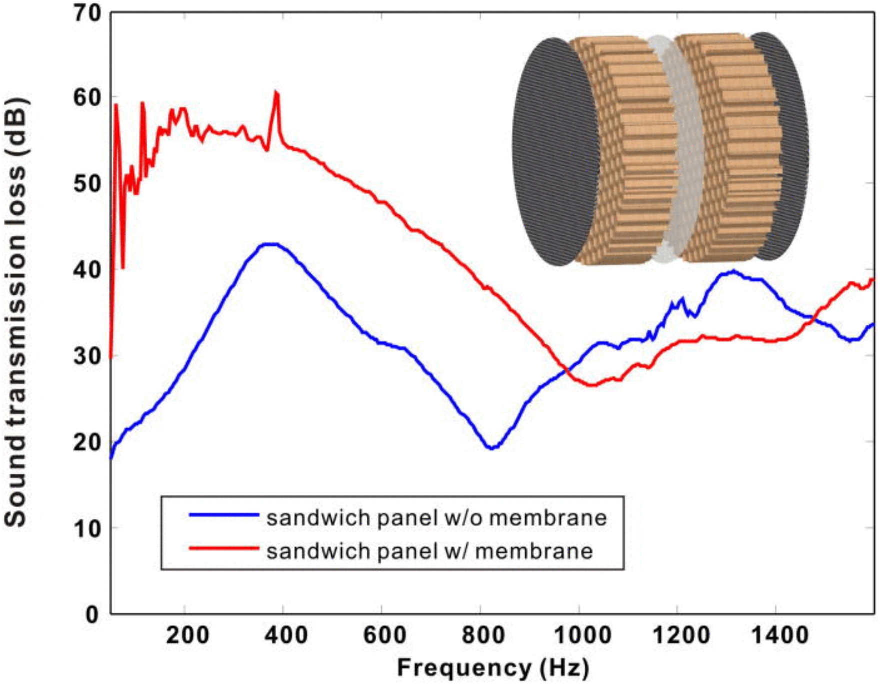

Ultrathin Sound Absorber at Work

Shahrzad Ghaffari
Mosanenzadeh

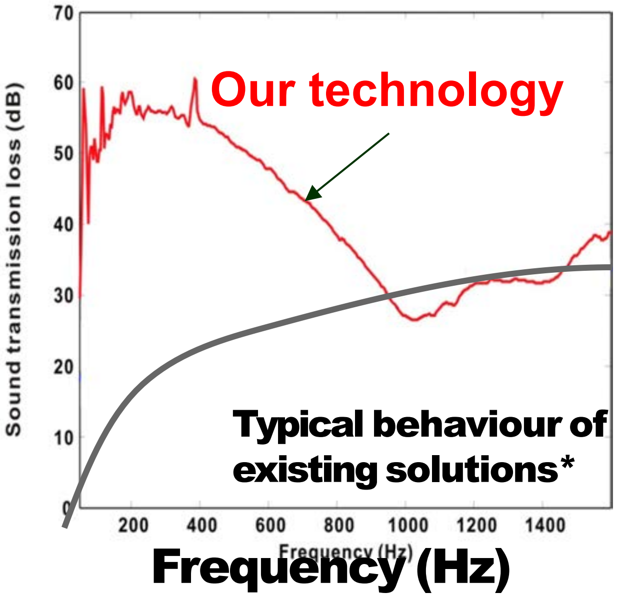

Before installation

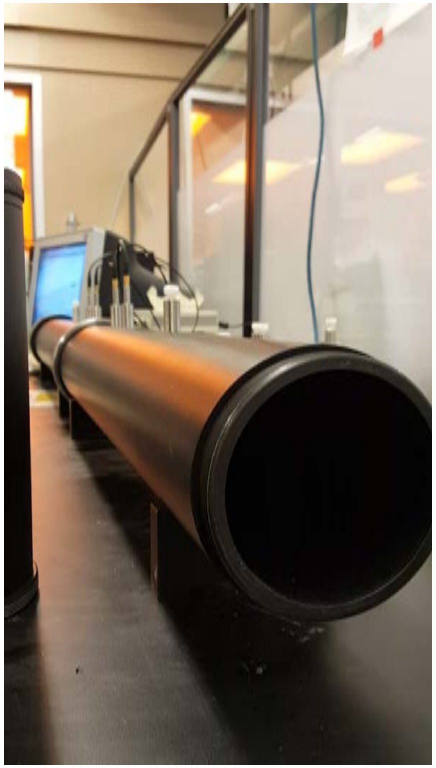

After installation

105 dB Noise

Strategies for Damping + Load Bearing

High stiffness But low damping

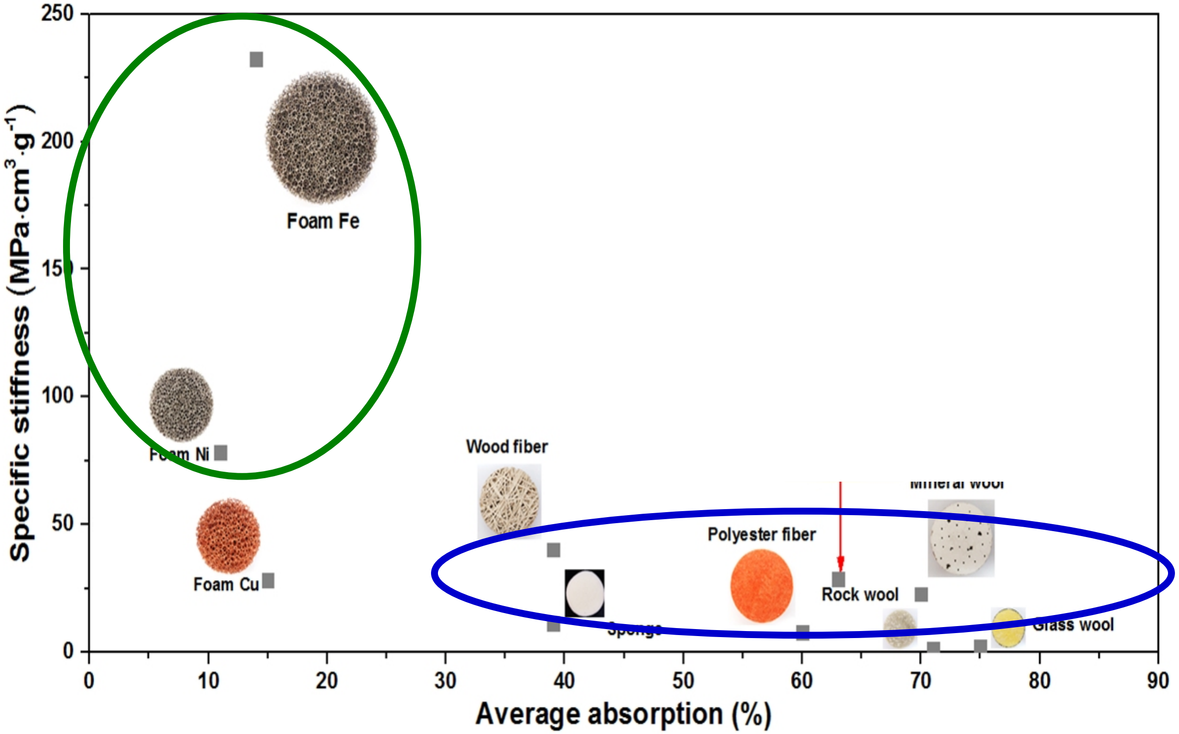

High damping But Soft

- The choice of the damping strategy is made based on the modal loss factors obtained on the treated structure.
- To compare efficiency of damping strategies applied on a loadbearing beam let's consider ***specific Young's modulus*** E/ρ as a function of loss factor of the structure.

Optimizing Absorption Efficiency + Load Bearing

In Collaboration with Juqi Ruan and Minghui Lu, Nanjing University

Porous
Cu Foam

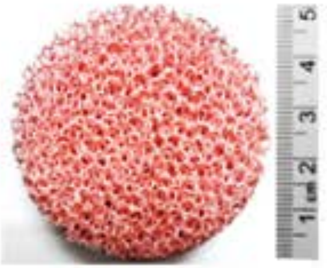

Cu/Silica Foam
by sol-gel coating

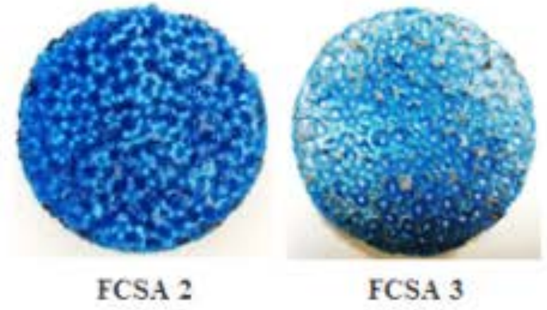

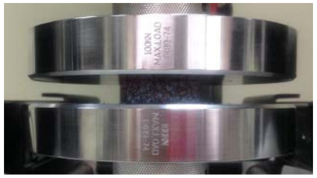

High
Mechanical
Strength

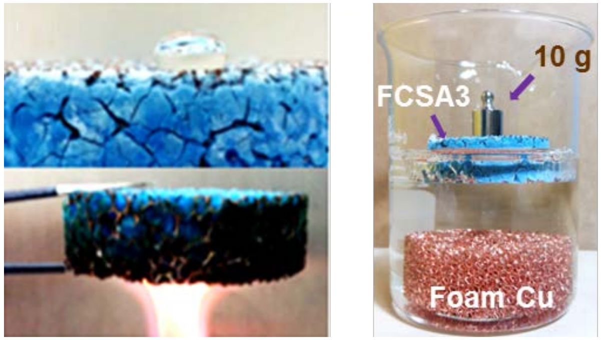

Hydrophobicity, inflammability
and light weight

Acoustic measurement data

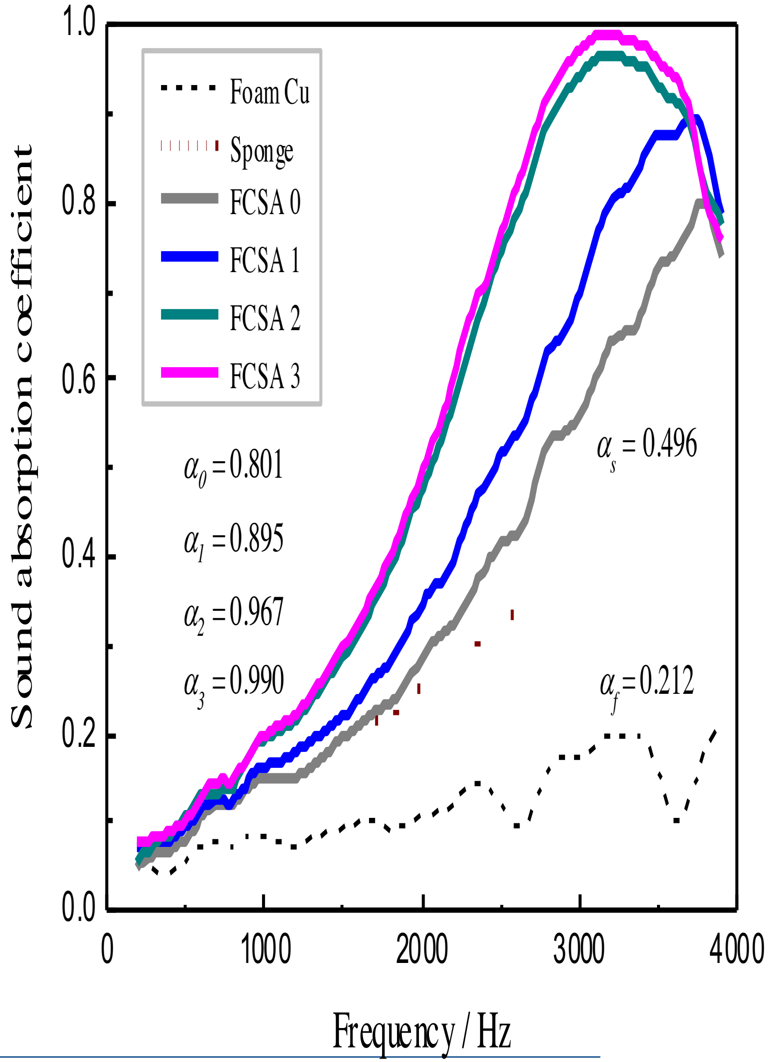

Bimodal Acoustic Model

Dr Shahrzad Ghaffari Mosanenzadeh

Chu Ma

A bimodal model is proposed to capture different pore size within the structure.

- Large pores of the copper foam are presented as a network of interconnected spheres.

- the aerogel is modeled as the porous absorber filling the primary structure using the poroacoustic model (Johnson-Allard-Champoux) with specified speed of sound.

Schematic 1

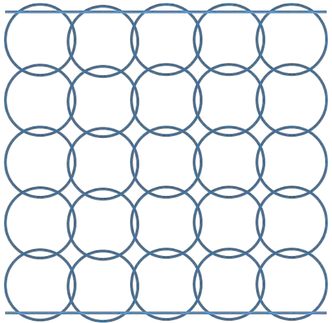

Schematic 2

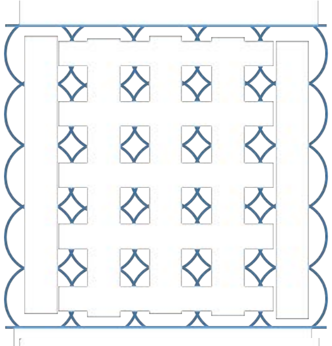

Schematic 3

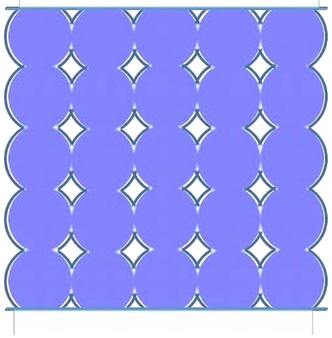

Bimodal Acoustic Simulation: Results

Bimodal simulation depicts the sound absorption of Copper/Aerogel composite foams accurately, showing the increasing trend of maximum absorption by increasing the amount of epoxy resin.

Table below compares the results from simulation with that of direct characterization, in terms of the peak values.

	Max. α		Frequency (Hz)	
Samples	Exp	Sim	Exp	Sim
FCSA-0	0.80	0.80	3780	3800
FCSA-1	0.90	0.88	3720	3700
FCSA-2	0.97	0.97	3180	3200
FCSA-3	0.99	0.99	3160	3200

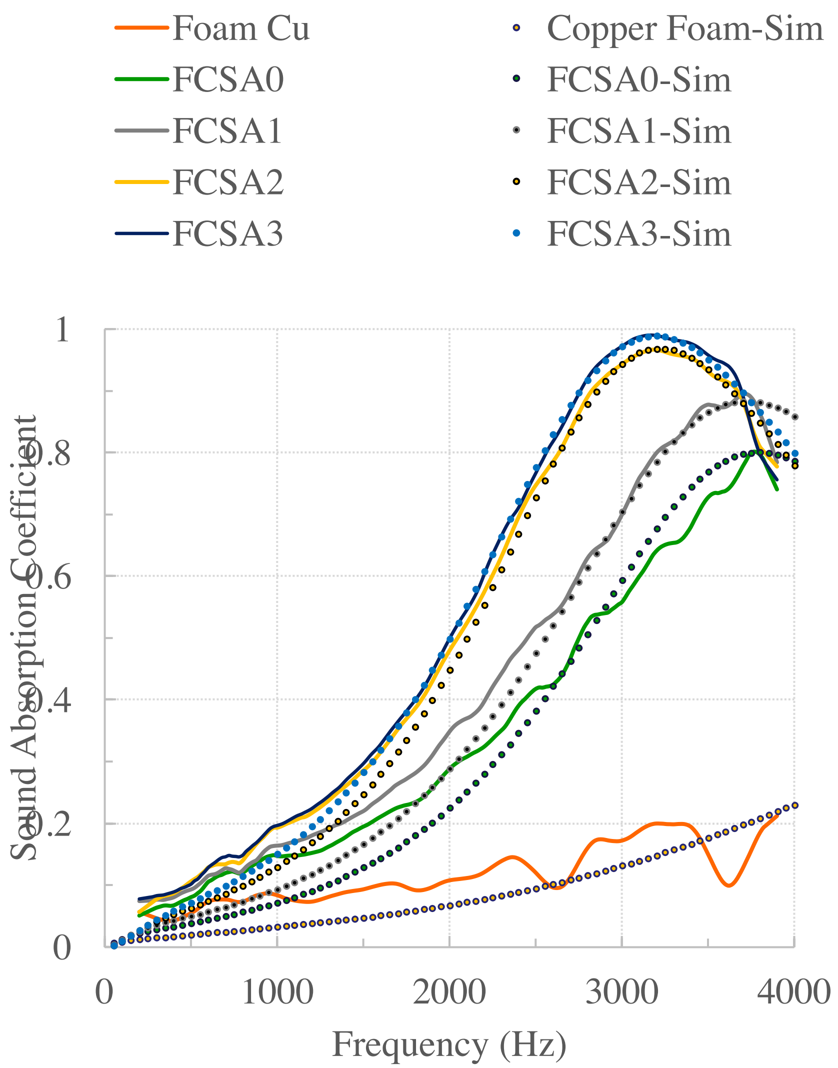

Juqi Ruan, Shahrzad Mosanenzadeh, Chu Ma, in preparation

Sound Dampening + High Stiffness: Novel Architectured Metamaterials!

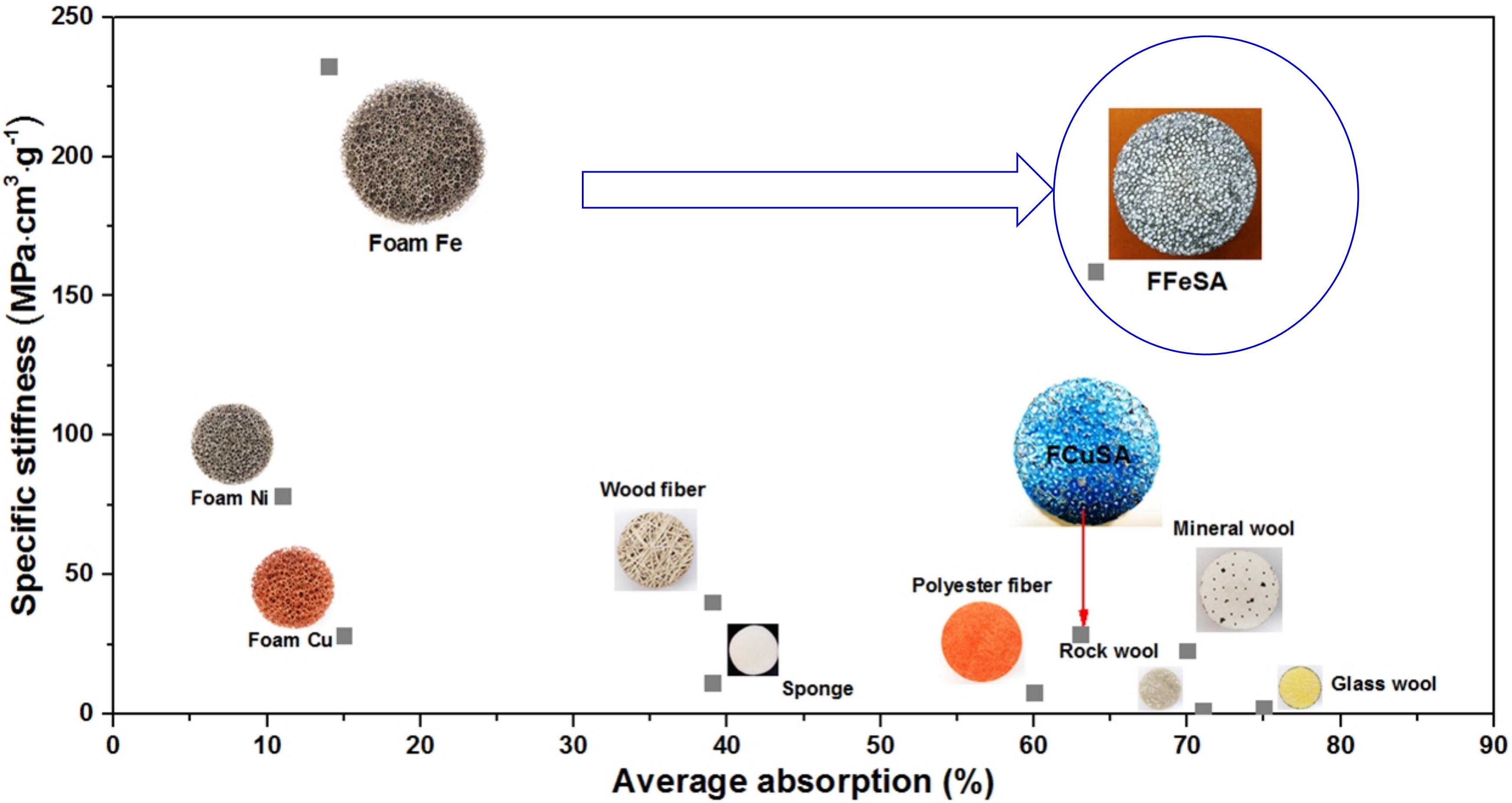

Juqi Ruan, Shahrzad Mosanenzadeh, Chu Ma, in preparation

Nonlocal Dynamics of Dissipative Acoustic Meta

Dr. Eunnie Lee

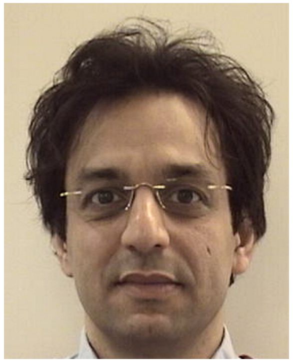

Dr. Navid Nemati

Development of nonlinear eigenvalue solver for acoustics

Nonlocality is important even in very simple subwavelength systems when compressibility is significant ($\nabla \cdot v \neq 0$) or when higher-order modes are concerned.

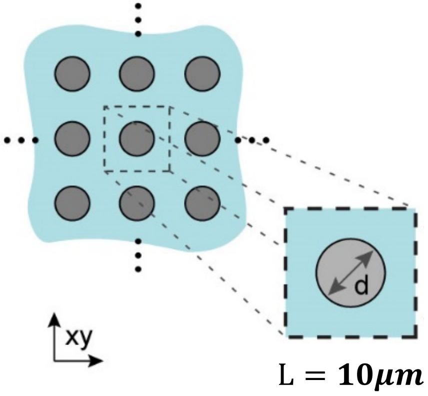

Fluid compression $|\nabla \cdot \vec{v}|$

excitation $\lambda = 400\mu m$

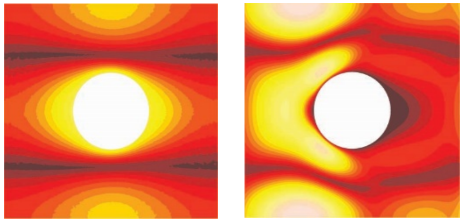

Mode 1 $\lambda_{\text{eff}} = 400\mu m$

Mode 2 $\lambda_{\text{eff}} = 13\mu m$

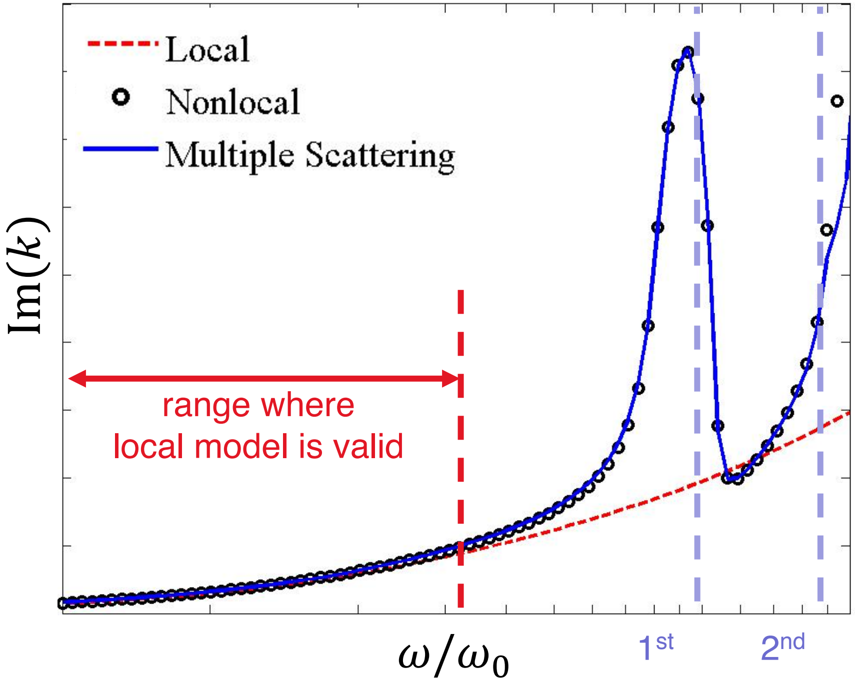

Nemati, Lee, Lafarge, Duclos and and Fang. PRB 2017

Outlook: Acoustic Meta Beyond Audible Frequencies

High fidelity
Speech/Voice recognition

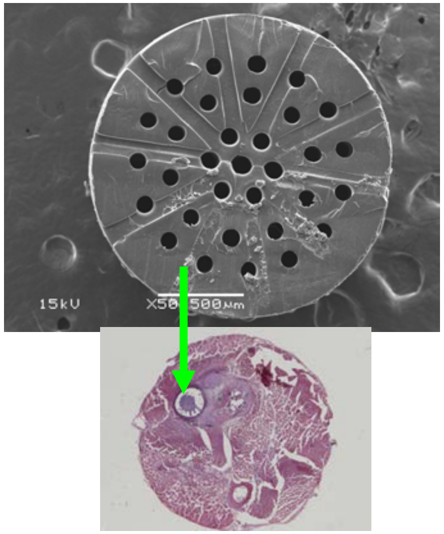

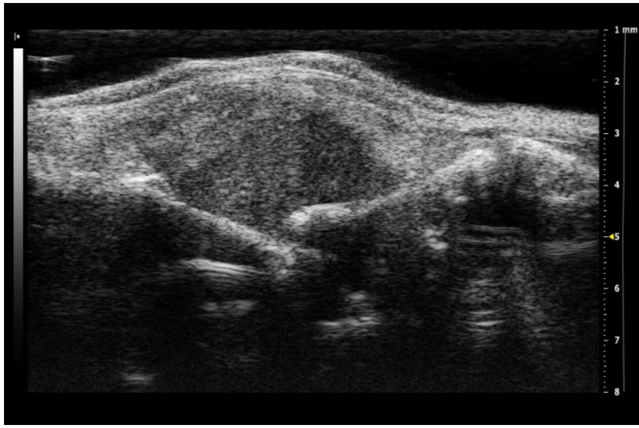

Ultrasonography

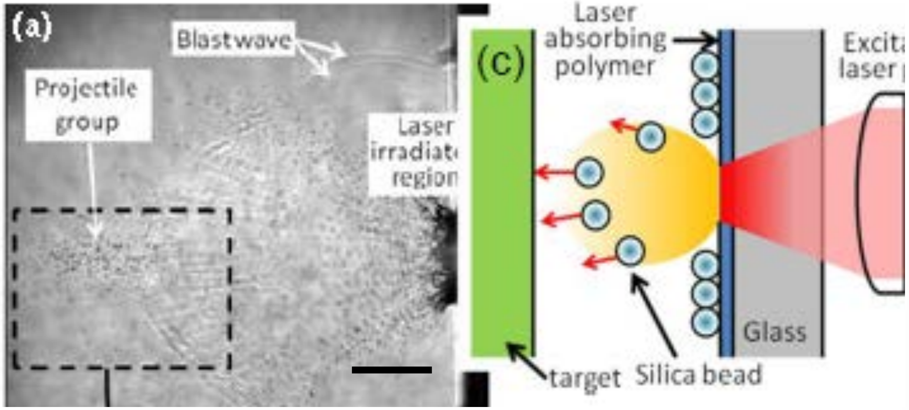

Laser Micro-shock wave

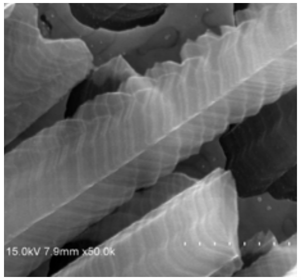

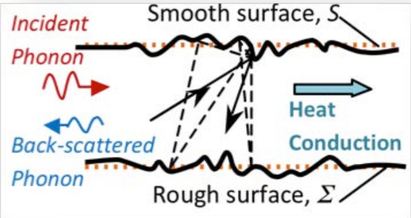

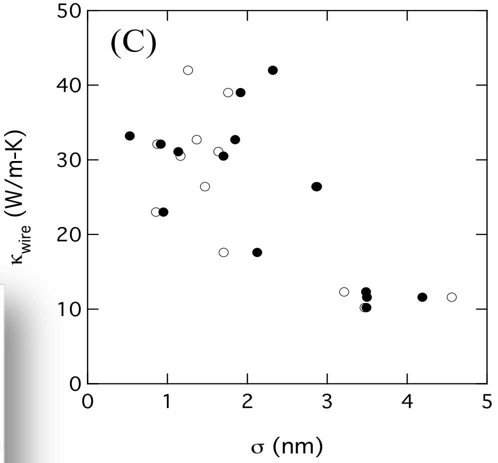

Rough Nanowires -> low conductance

Optically and Sonically Camouflaged Hydrogel

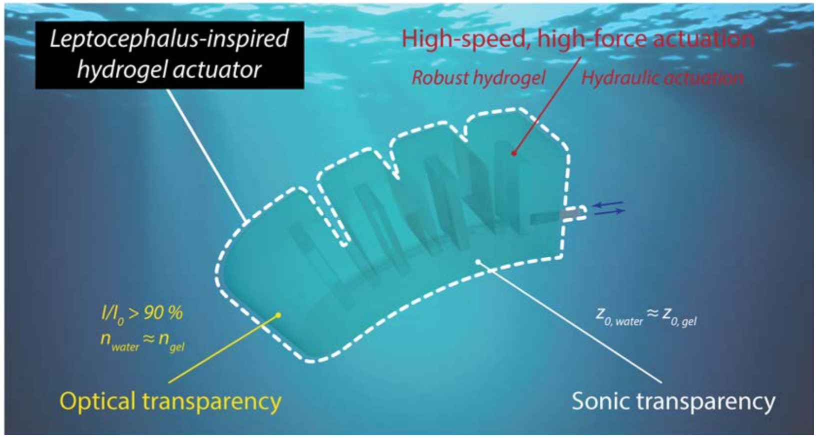

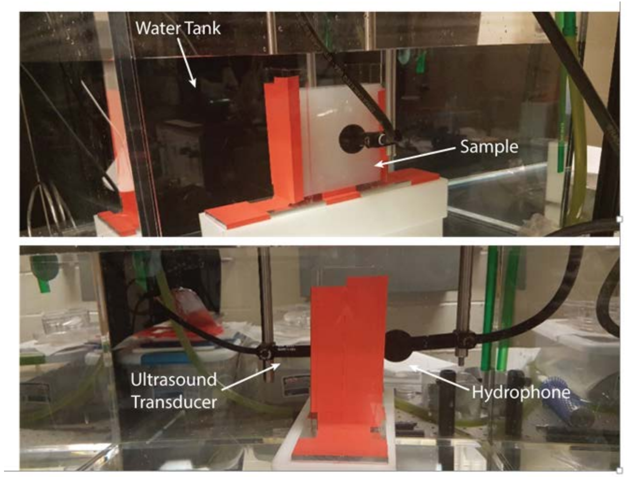

	Water	Hydrogel	Ecoflex	Elastosil	Sylgard 184
optical n	1.333	1.337	N/A†	N/A†	1.423
I/I_0	100 %	> 90 %	< 5 %	< 0.1 %	> 90 %
c [$\mathrm{m \cdot sec^{-1}}$]	1448	1486	983.4	979.6	1022
z_0 [MPa·s/m]	1.448	1.487	1.052	1.058	1.053
R	0	0.013	0.158	0.156	0.158

H Yuk, S Lin, C Ma, M Takaffoli, NX Fang, X Zhao,Nat. Commun. 8, 14230 (2017)

Molding the Flow of Waves: Transformation Optics

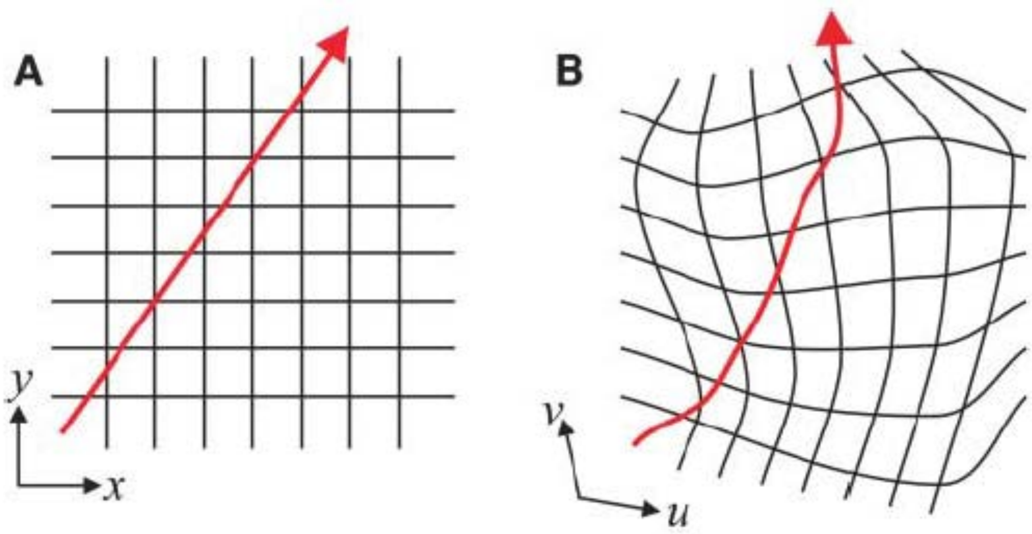

Free space field

Distorted field

J. B. Pendry et al, *Science* 321,2006

$$
\begin{cases}
\beta_1 = \dfrac{\mathbf{A}\beta_{1'}\mathbf{A}^T}{\det \mathbf{A}} \\
\rho_1 = \dfrac{\mathbf{A}\rho_{1'}\mathbf{A}^T}{\det \mathbf{A}} \\
\beta_2 = \dfrac{\mathbf{A}\beta_{2'}\mathbf{A}^T}{\det \mathbf{A}} \\
\rho_2 = \dfrac{\mathbf{A}\rho_{2'}\mathbf{A}^T}{\det \mathbf{A}}
\end{cases}
$$

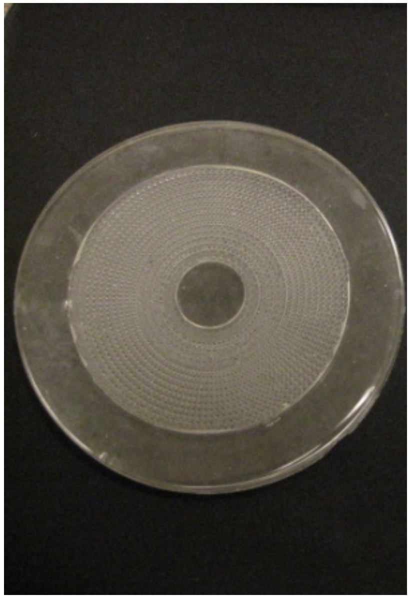

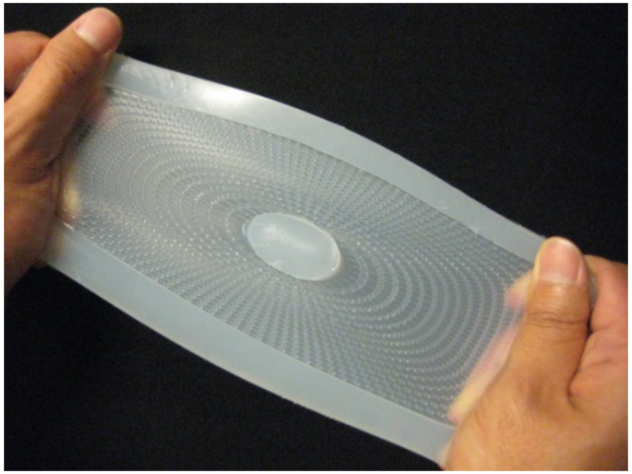

Similar Notation in Solid Mechanics:

A :the deformation gradient tensor

Application Example: Broadband Bi-functional Acoustic Metalens

Collaboration with Hongshen Chen group, ZJU

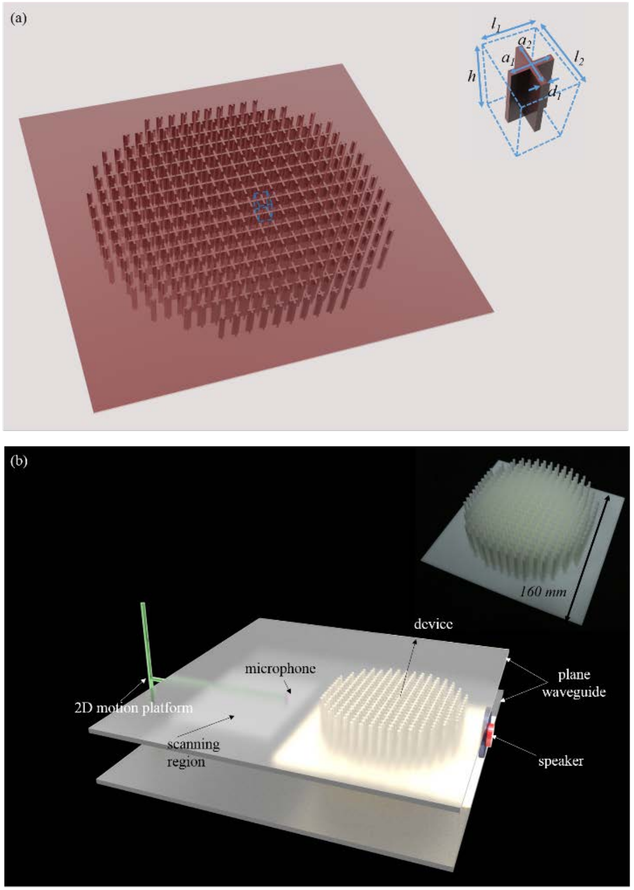

Left: Luneberg lens

Top: Maxwell-fisheye lens

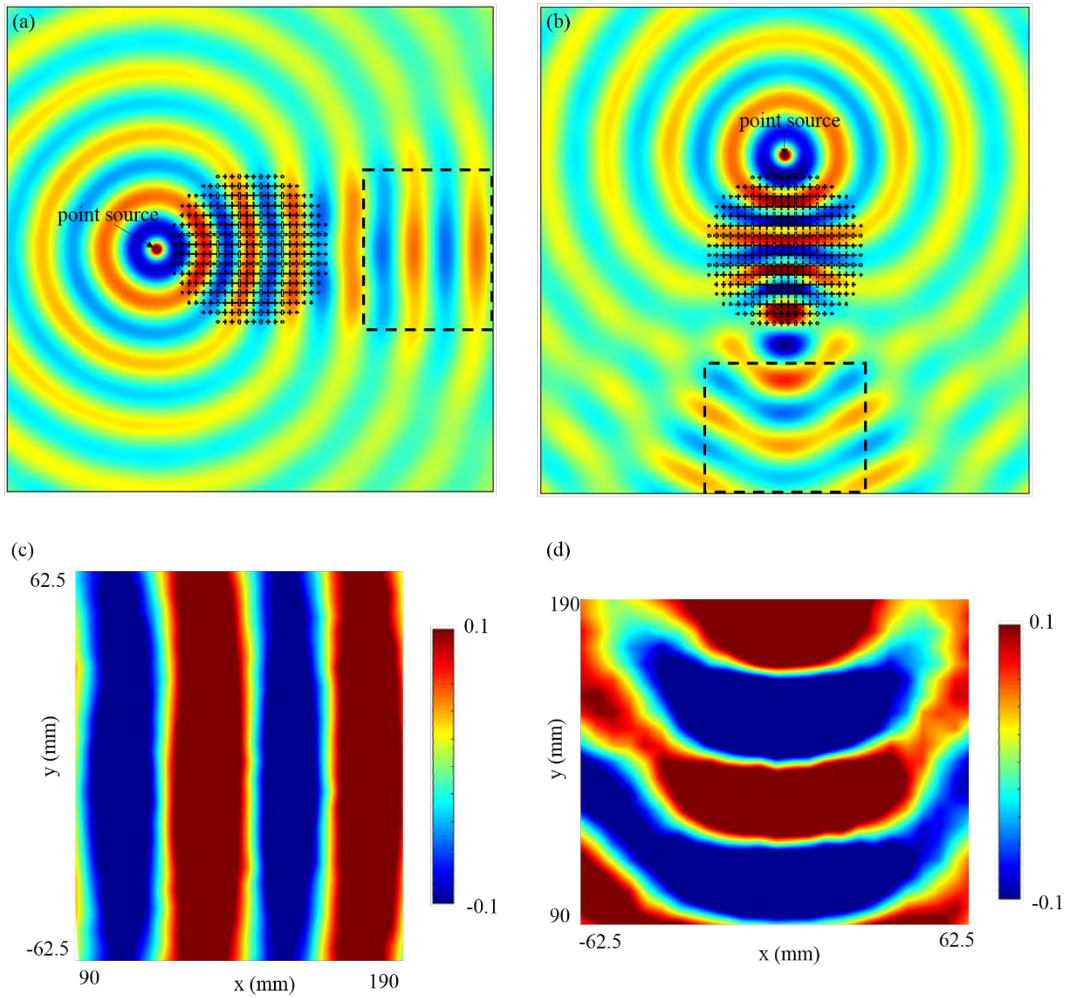

Rongrong Zhu, Chu Ma, et al, APL, 2017

Future: Metalens for λ/40 Sound Focusing

AA Maznev, G Gu, S Sun, J Xu, Y Shen, N Fang, S Zhang, New Journal of Physics 17 (4), 042001, 2015

Experimental Configuration

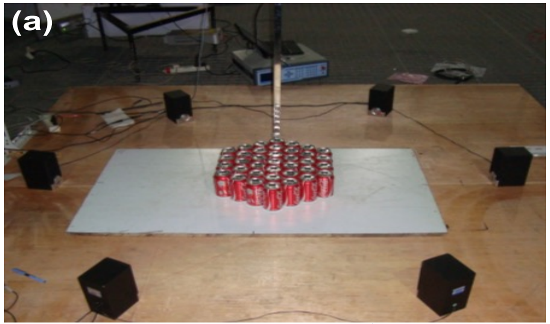

Analytical Model

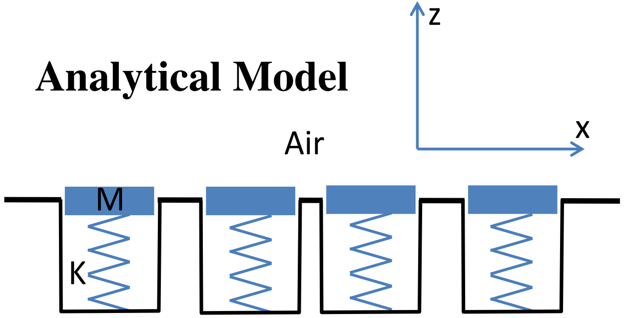

Dispersion Relation

$$\left(k^2-\frac{\omega^2}{c^2}\right)^{1/2}(\omega_0^2-\omega^2)=\frac{\omega^2 FA}{M}$$

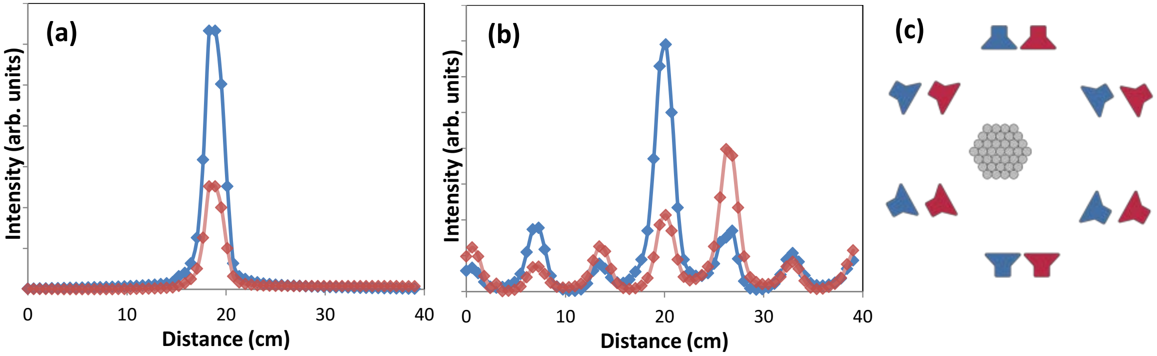

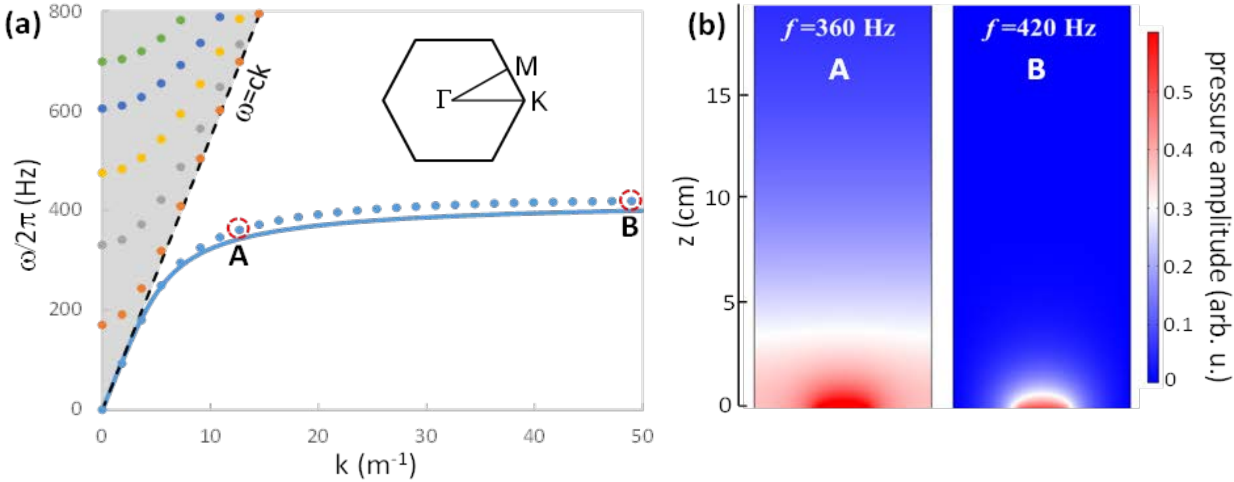

Outline

- **Acoustic Meta-materials:**

  Quest for Thin Absorbers and Metalenses

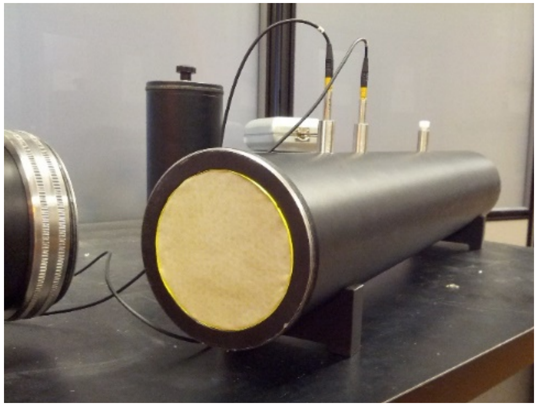

- **Micro/Nano Fabrication for Metamaterials**

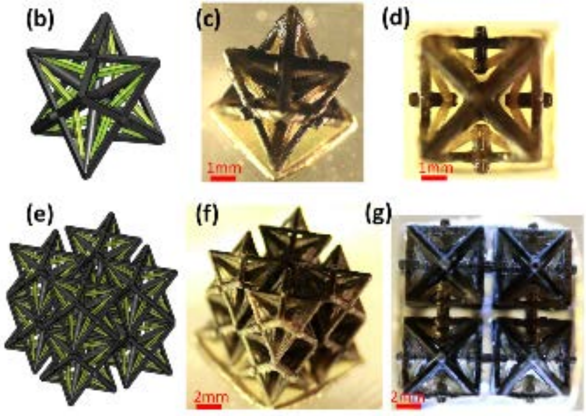

Overall Strategy:
Design and Testing of 3D Functional Materials

FEEDBACK TO DESIGN AND FAB

Analytical design

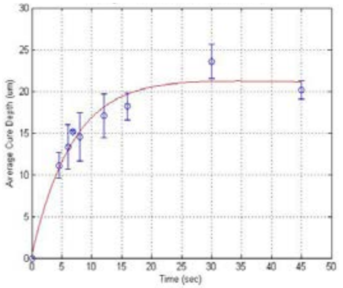

Computational optimization

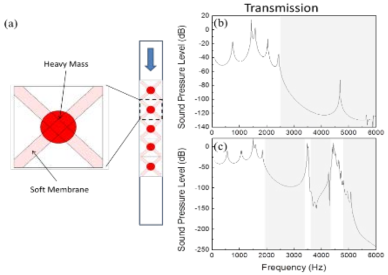

"DESIGN IT"

Multimaterial Fabrication

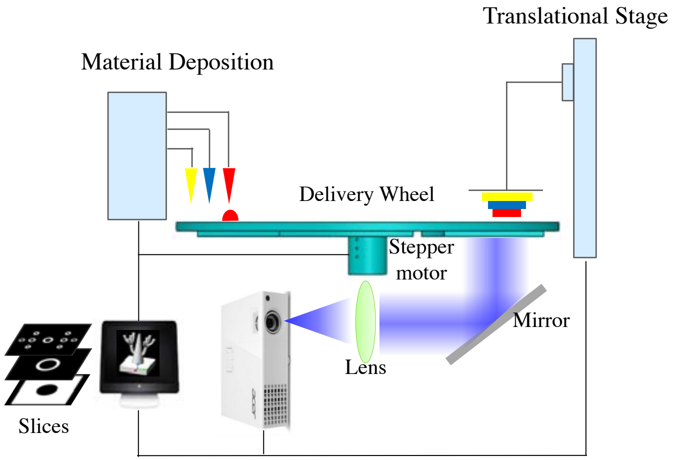

"BUILD IT"

Mechanical/ Acoustic Testing

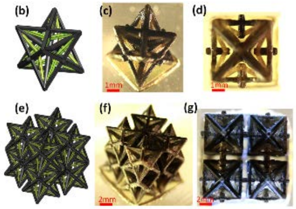

solid polymer

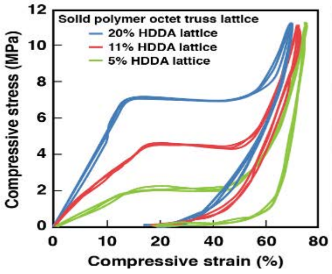

"TEST IT"

Multi-material stereolithography system

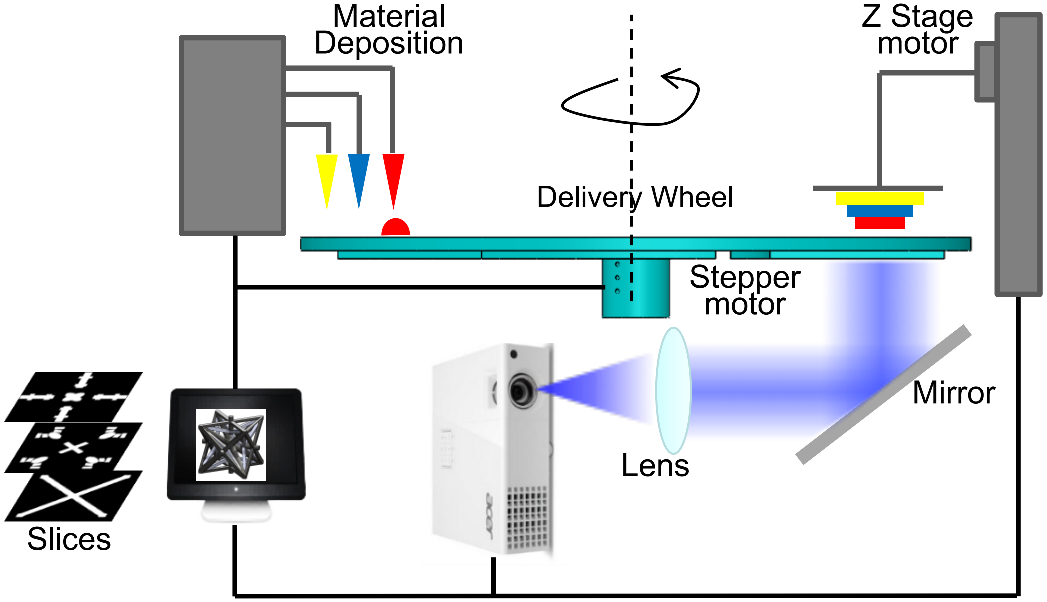

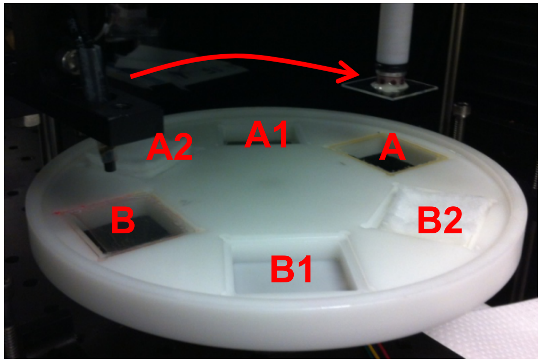

A: window for material A
A1: ethanol for material A
A2: cotton for material A
B: window for material B
B1: ethanol for material B
B2: cotton for material B

Technique: multimaterial stereolithography

✓**Capability**: composite structures, arbitrary 3D geometry, resolution <15 *μ*m

✓**Different Components**: up to 3

✓**Materials**: hydrogel, elastomer, plastic, metal

✓**Activation**: magnetic, electric, thermal, light

Examples of 3D Microscale Components

On chip Tissue culture

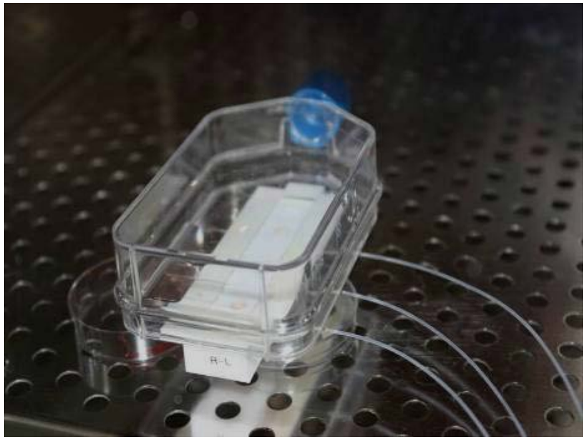

Biomedical microdevices 11,1309 (2009)

Ceramic meshes

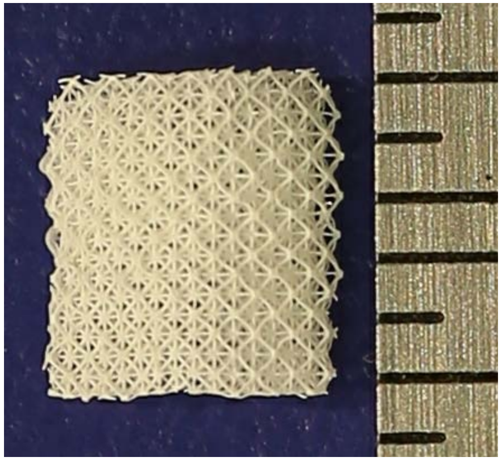

Complex microlenses

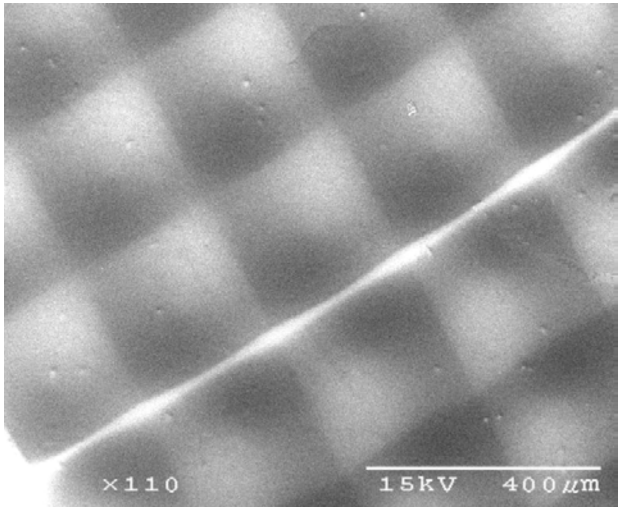

Shape memory polymers

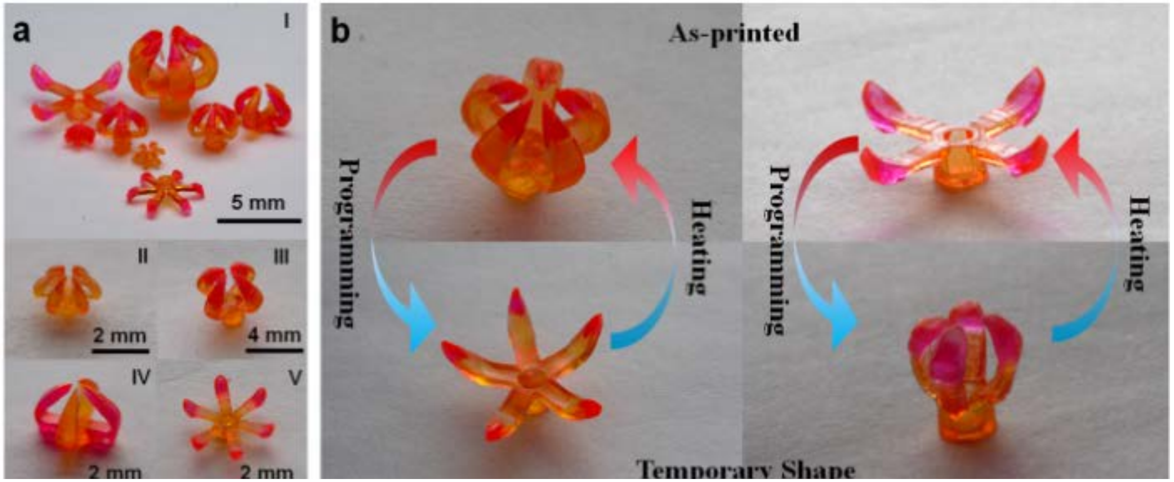

Qi Ge, et al, Scientific Reports 6, 31110, 2016

Post-Processing

PµSL – template polymer micro-lattice (solid polymer)

Hydrostatic Sintering

Solid ceramic

- 1300° C for 2 hrs
- 20% vol. shrinkage

600 mesh, 23 micron

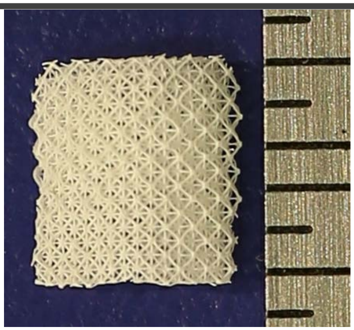

Electroless plating

Hollow metal

- Ni-P coating
- t: 30 nm ~ 2 µm
- polymer thermal decomposition

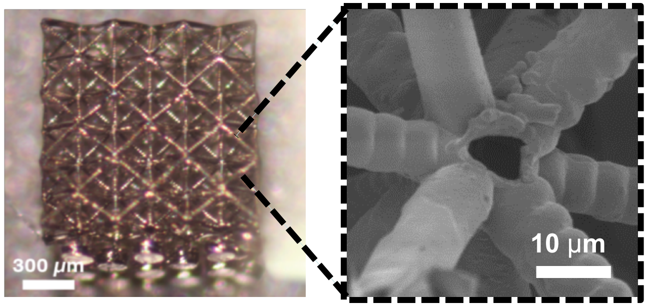

Atomic Layer Deposition (ALD)

Hollow ceramic

- Al_2O_3 coating
- t: 2 nm ~ 300 nm
- polymer solvent removal

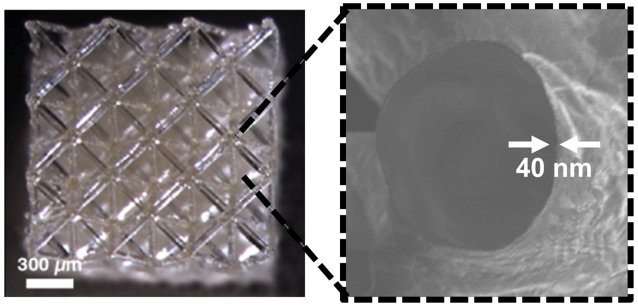

Relative density spanning over **4 decades**

Comparison of Different Microscale Printing

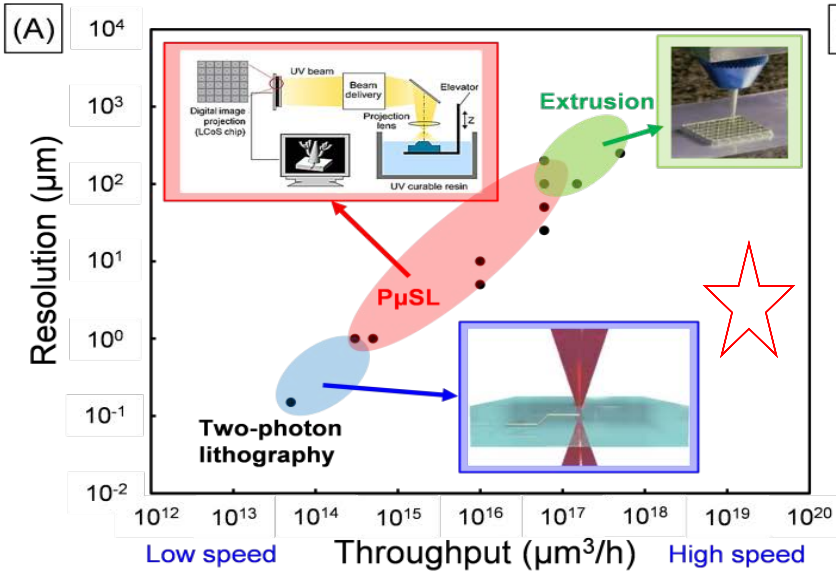

Single Exposure fabrication of 3D STRUCTURES

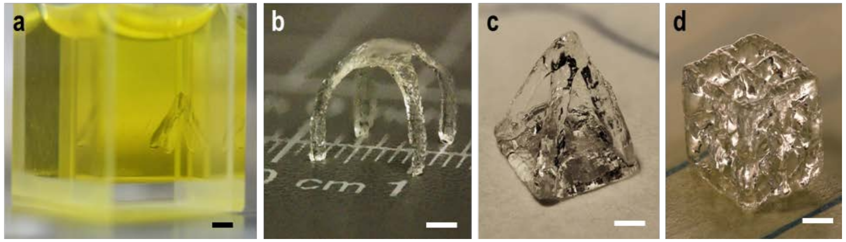

Shusteff et al, SFF conference, Austin, Aug, 2016

	PuLSE	Jet / FDM	SLS
Resolution	100nm to >50um	1-200 um	6-500um
Gelation methods	Photo	Photo, chemical, thermal, shear thinning	thermal
Materials Viscosity	1–300 mPa/s	8 mPa·s to >6 × 10^5Pa·s	-
Fabrication speed	Medium to high (depending on resolution)	Low	Medium
Cyto viability	45-90%	75-95%	-

Volumetric Single-Exposure 3D Fabrication

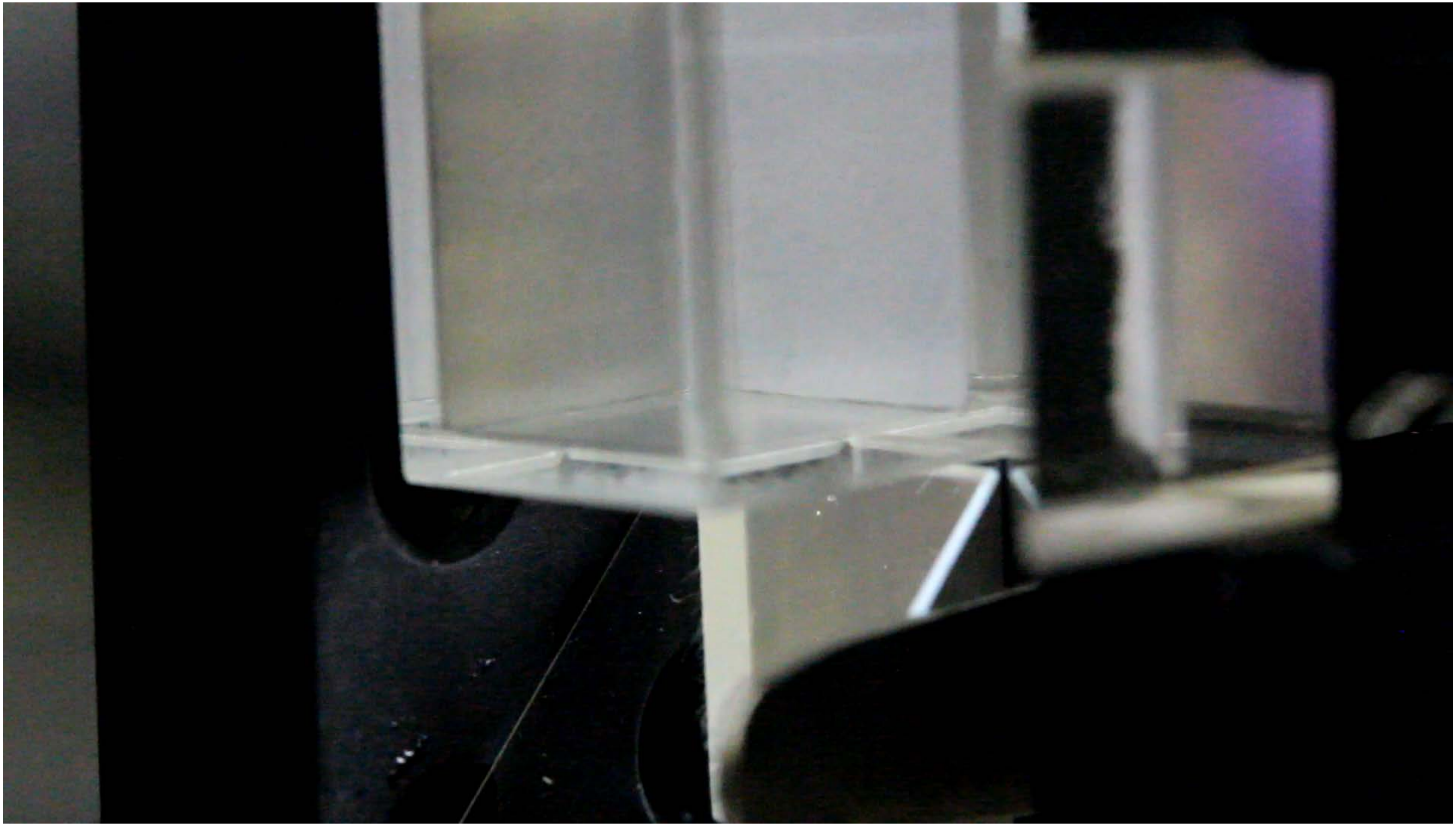

Maxim Shusteff, et al, accepted, in press, 2017

Complex Functional Voxels For Lightweighting

We have been using a new software package called Netfabb

Unit cell design

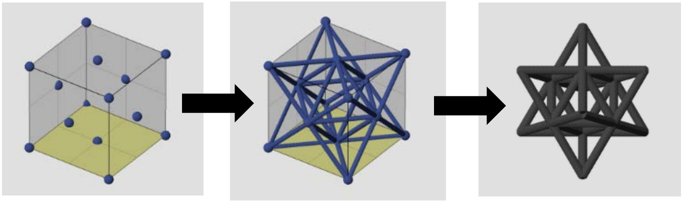

Infill object with cells to form lattice

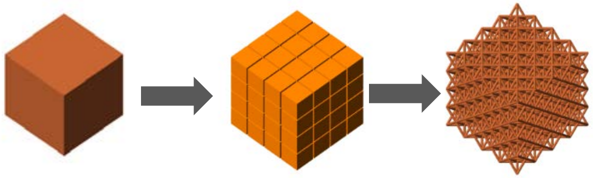

Conform lattice to surface

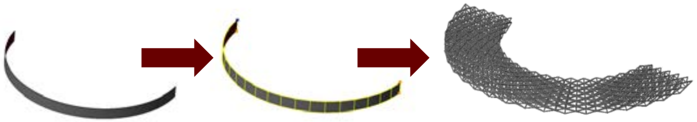

Convert finished part to slices of desired thickness

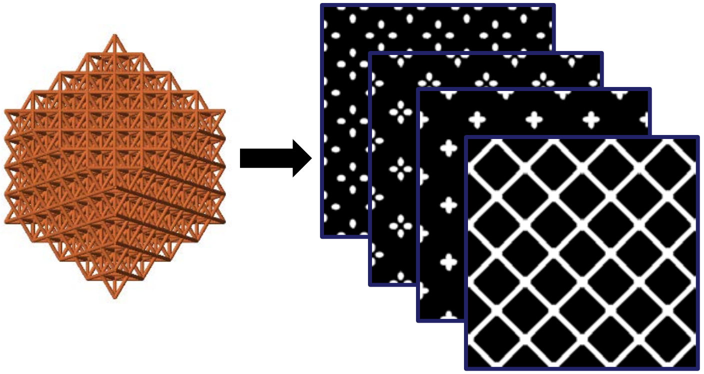

Light Weight and Load Bearing

37 g weight (160,000 times of the weight of the structure's)!

- Uniaxial compression test

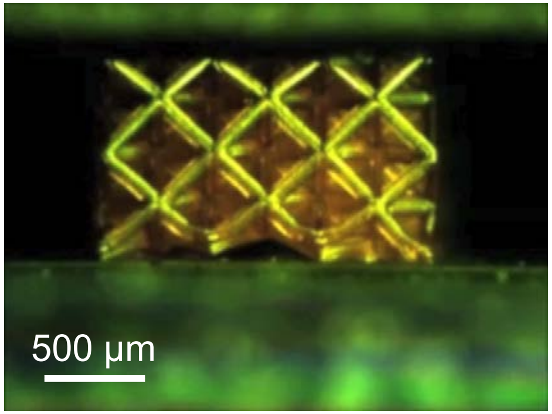

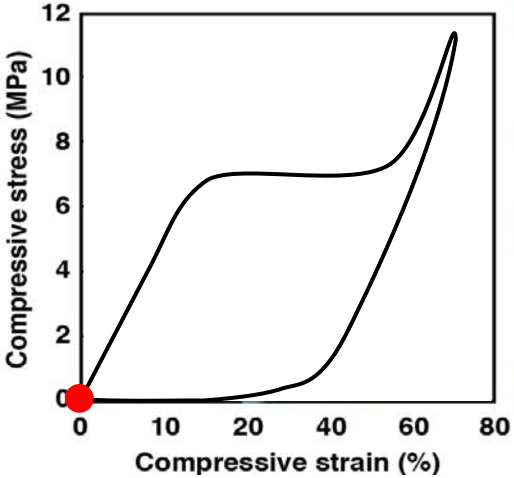

- Representative data

solid polymer

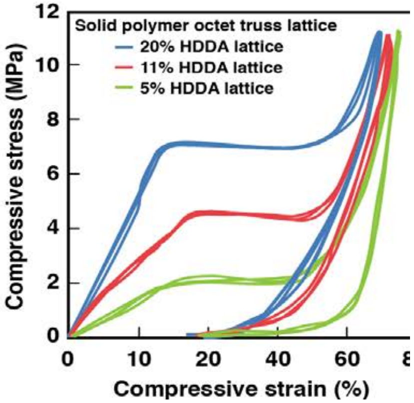

hollow metal

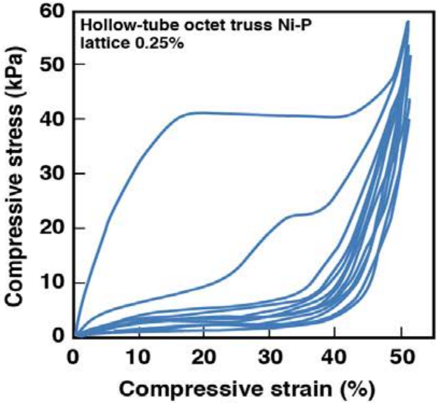

hollow ceramic

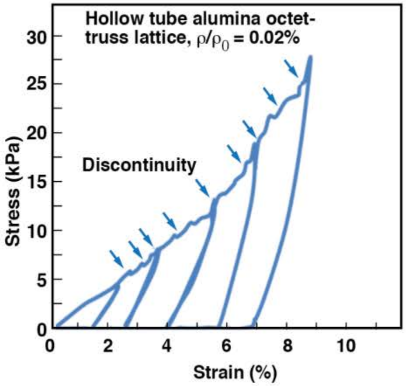

Architectured Metamaterials with Superior Ductility

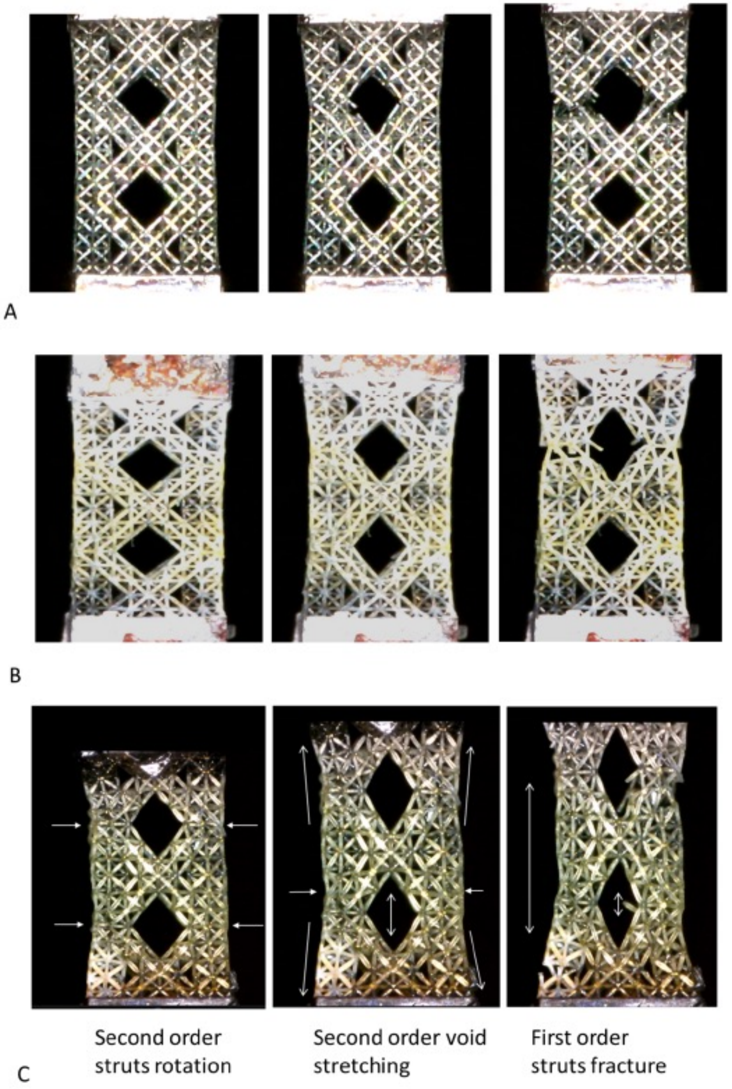

Second order struts rotation

Second order void stretching

First order struts fracture

Strength as a function of relative density of optimal stretch-dominated multi-scale metamaterials compared to other low density materials

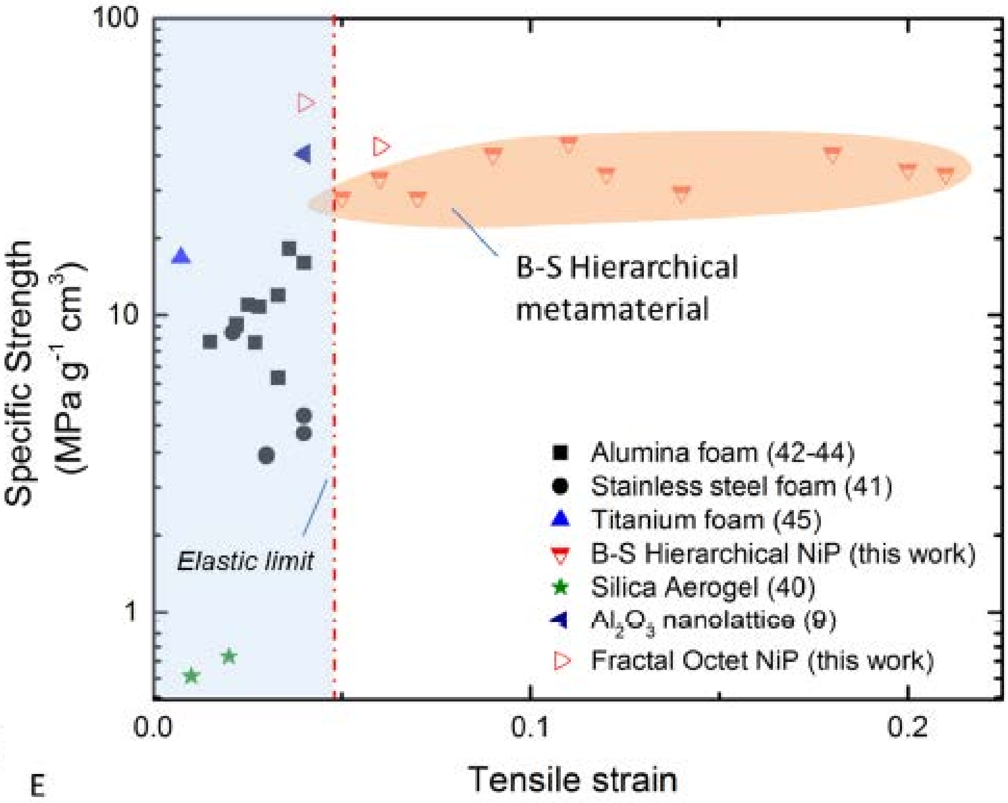

X. Zheng, N. Fang, et al, Nature Materials. 2016

Tunable CTE Materials: Preliminary Experiments

measurement confirmed large negative thermal expansion ($2.9 \times 10^{-5} K^{-1}$) over a large range of temperature (350K-524K)

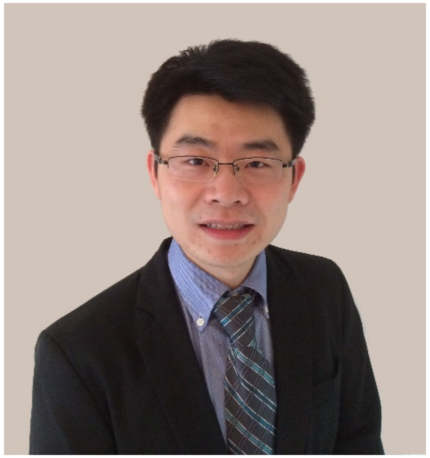

Dr Qiming Wang (USC)

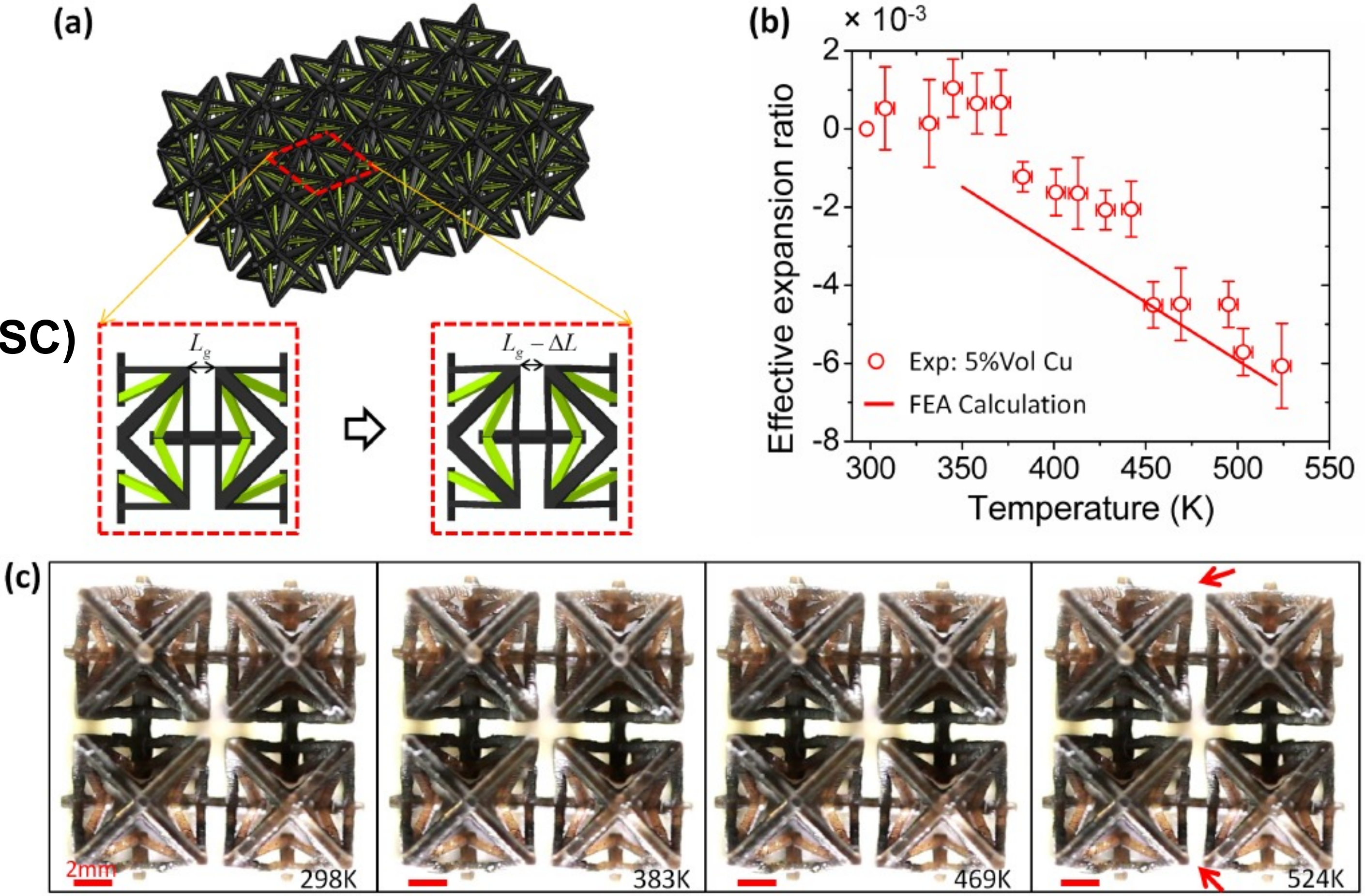

Q. Wang, et al, Physical Review Letters, 2016

Future Sound Voxels:
Computational Design and Fabrication

A Library of Digital Acoustic Metamaterials

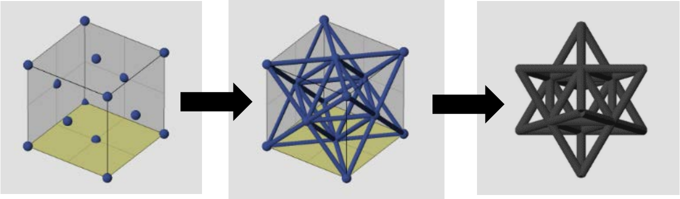

Tailored Physical Properties
(thermal expansion,
conductivity,
permittivity etc)

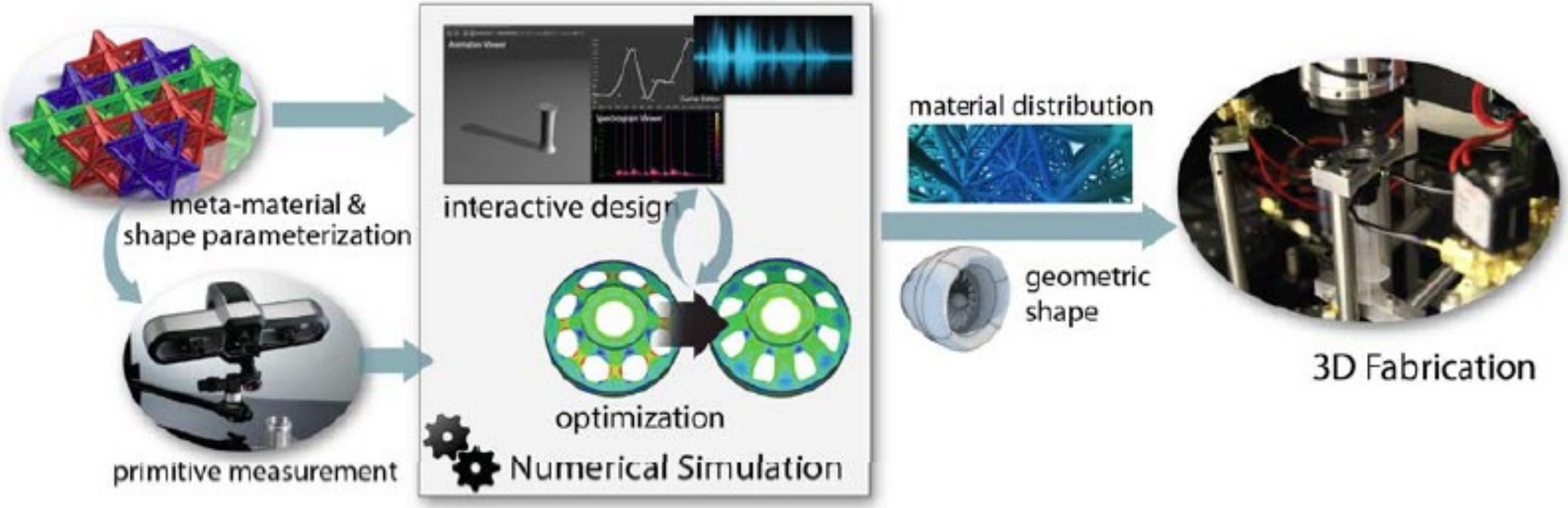

新的环保隔音技术:国际产学研合作

DESIGN FOR NOISE REDUCING MATERIALS & STRUCTURES

DENORMS

COST Action CA15125

cost
EUROPEAN COOPERATION IN SCIENCE & TECHNOLOGY

Funded by the Horizon 2020 Framework Programme of the European Union

Chair: Mr Jean-Philippe GROBY (FR)
Co-Chair: Dr Olga UMNOVA (UK)

Thank you for your attention!

Thermomechanical mismatch: A Challenge Problem

Optical and RF assemblies

Catalytic Converters

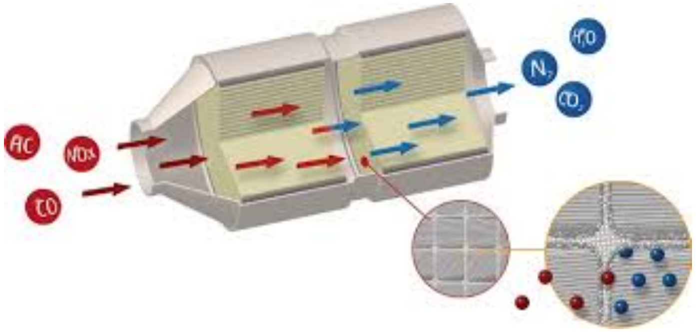

Medical implants

Material Requirements for Optical Mount	
Gradient in CTE	<8.5 µstrain/K
Density	< 3 g cm^{-3}
Operating temperature	-54 to 70ºC
Thermal Conductivity	>25 W m^{-1} K^{-1}

By developing materials that have tailored material properties (CTE and Young’s Modulus), an optical mount can be made that is stable under different operating conditions with reduced weight, complexity, and improved performance.

Strategies for negative thermal expansion

1. Design molecular structures

Geometric rotation of units to sustain temperature increase

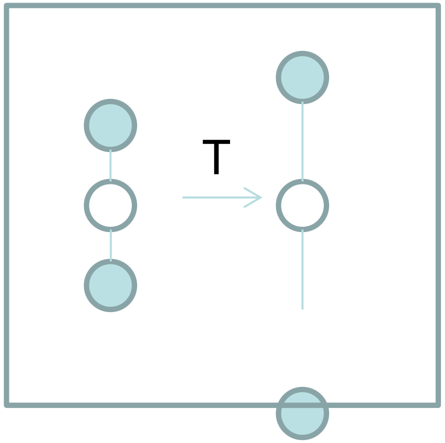

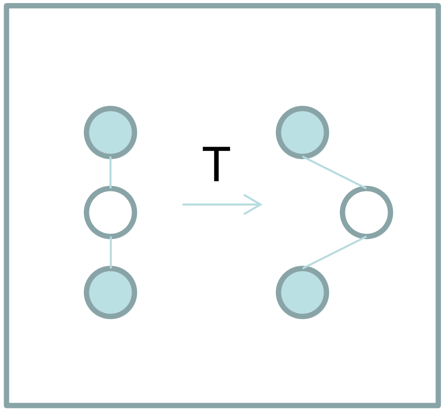

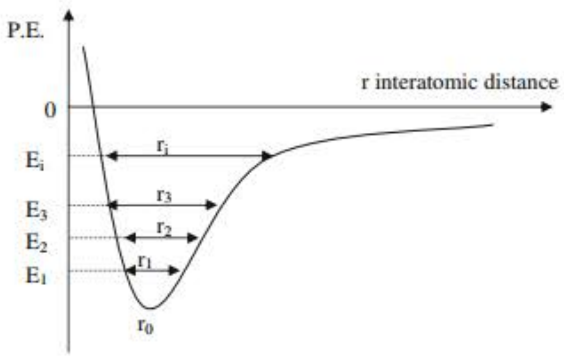

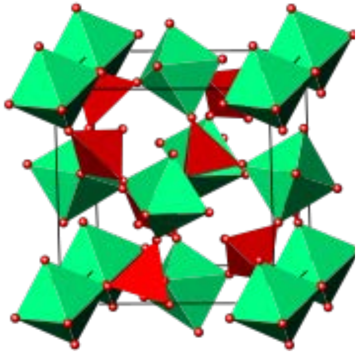

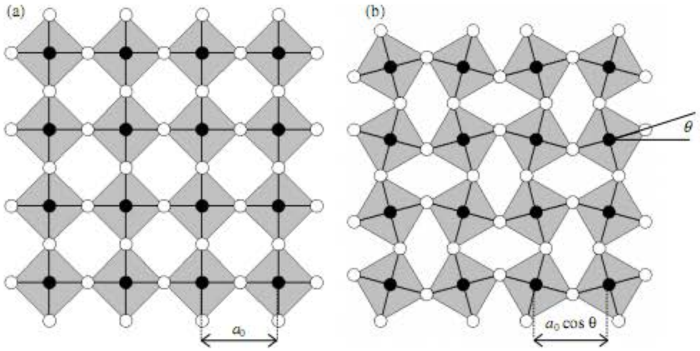

Zr(WO4)2

$SrCu_3Fe_4O_{12}$

Miller, W., et al. *Journal of materials science* 44.20 (2009): 5441-5451.

Lind, C., 2012. Materials 5, 1125-1154.

Takenaka, K., 2012. Science and Technology of Advanced Materials 13, 013001.

Need of Novel Materials beyond Ashby Chart!

- Expand usable space on material selection chart for thermal expansion vs. stiffness

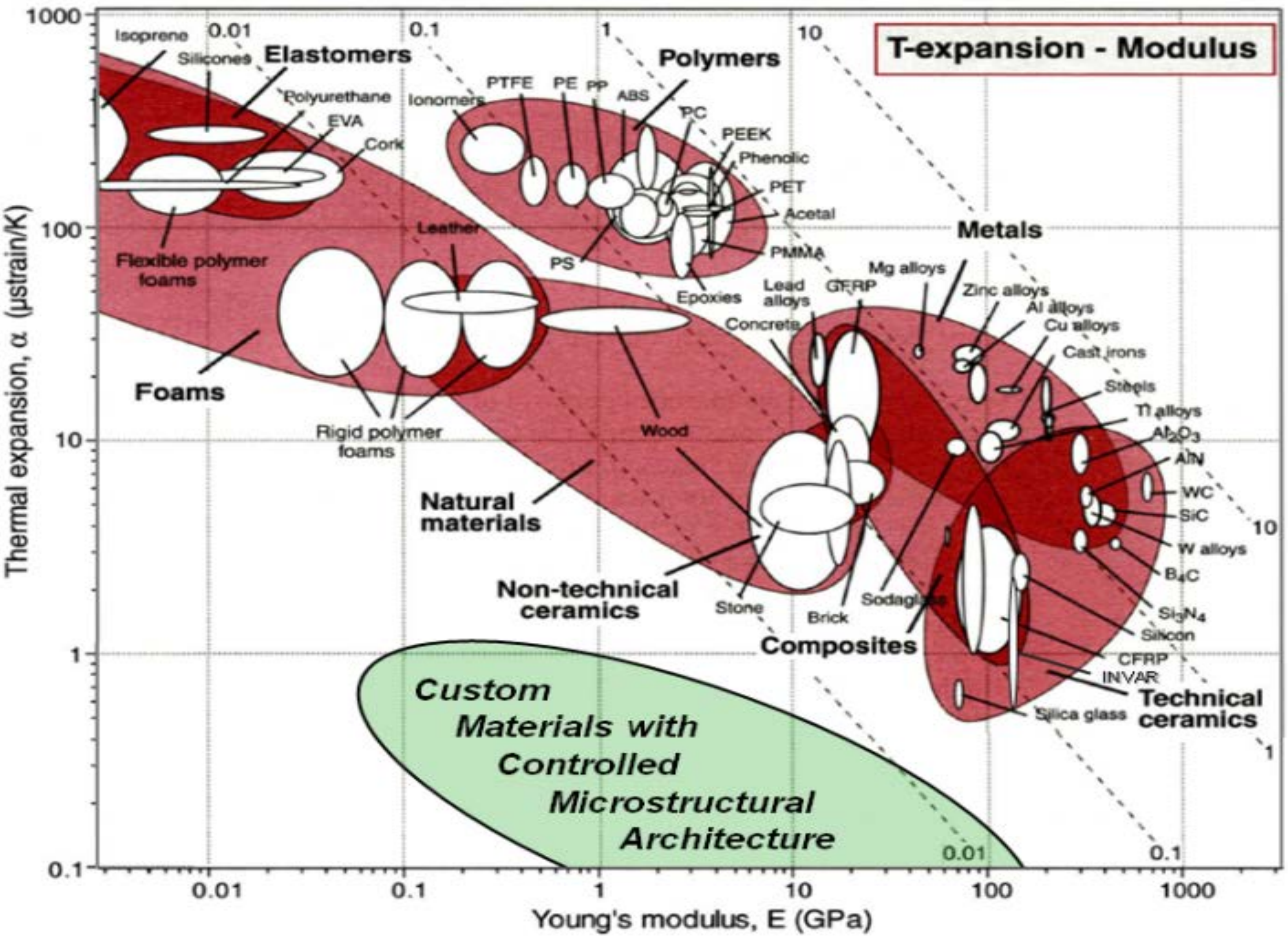

Strategies for negative thermal expansion

2. Bi-material Unit Cells with Free Volume

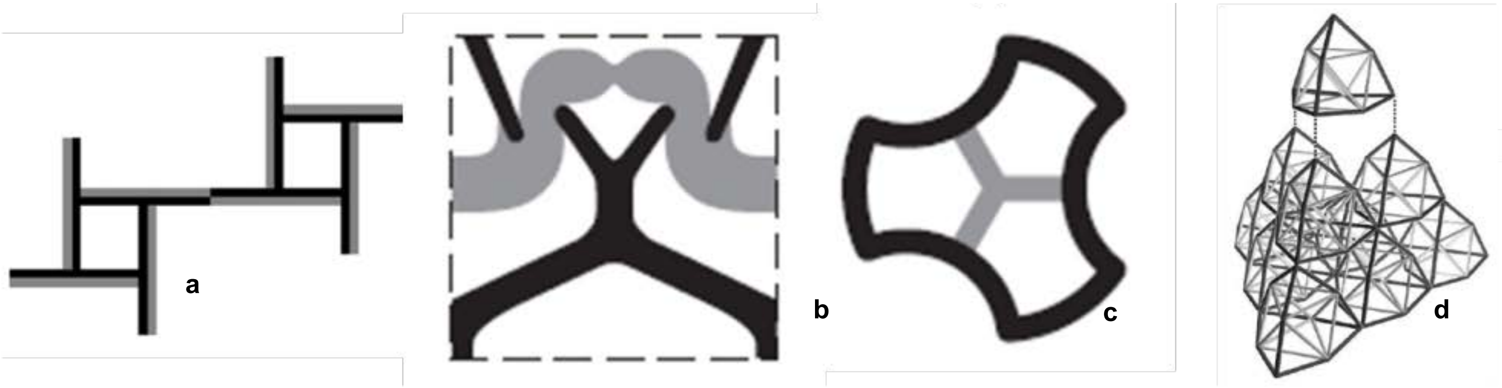

- Heterogeneous structures of materials with dissimilar thermal expansion coefficients and void space theoretically exhibit ultra-low thermal expansion.
- Unit cell geometries can be assembled into 2-D and 3-D lattices to form “bulk” material with ***designed*** properties.
- Architectural design and fabrication control at the microscale will enable this breakthrough.

a) Lakes, R., 2007, Applied Physics Letters, 90, 221905
b) Sigmund and Torquato, 1997, JMPS, 45(60), 1037-1067.
c) Jefferson *et al., 2009,* International Journal of Solids and Structures 46(11-12):. 2372-2387.
d) Steeves *et al.2007,* JMPS, 55: 1803-1822.

Tunable CTE Materials: Preliminary Design

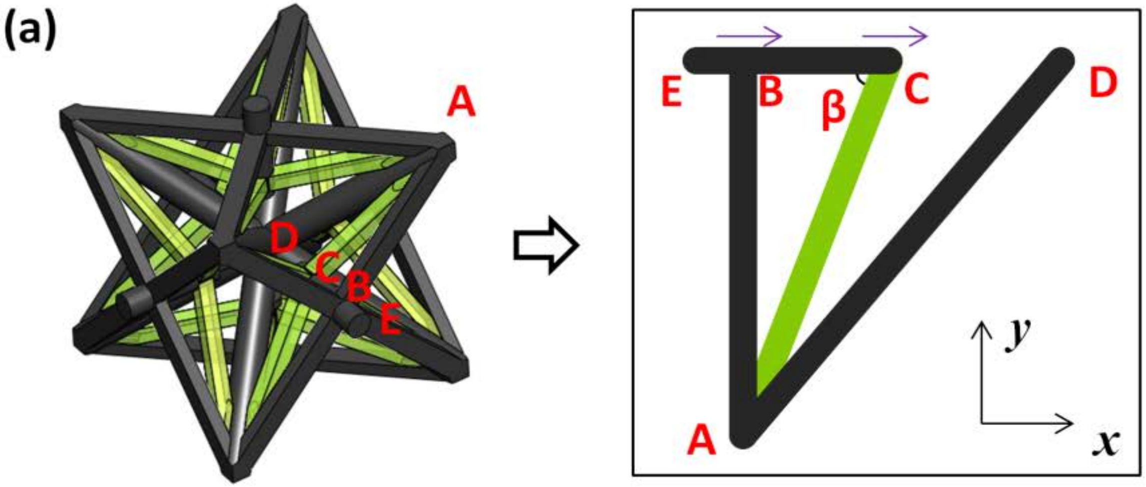

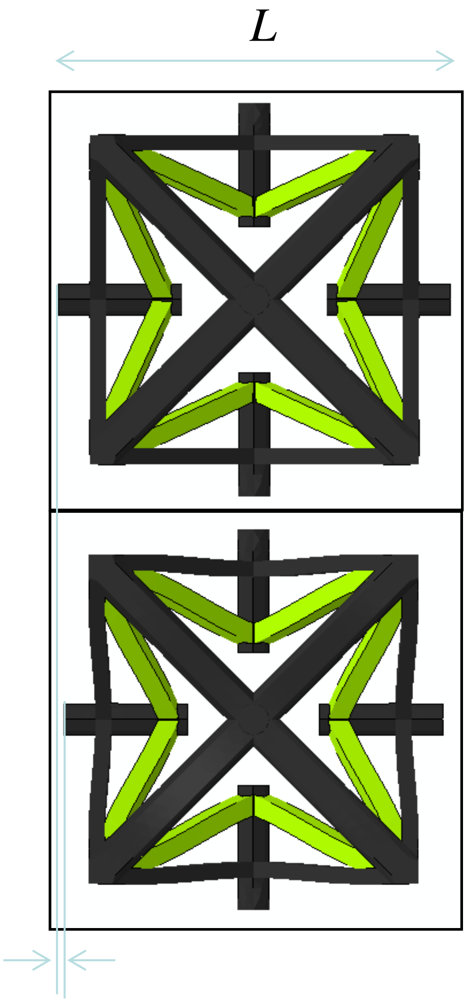

Approximated displacement of node E:

$$d_E \sim \frac{\alpha_1 \Delta T L_{AC}}{\cos\beta} - \alpha_2 \Delta T \left(L_{BC} + L_{BE}\right)$$

The effective expansion ratio:

$$\boxed{\eta \sim -\frac{2d_E}{\sqrt{2}L_{AB}} = -\sqrt{2}\Delta T \alpha_1 \left(\frac{2}{\sin 2\beta} - \frac{k}{\tan\beta} - \frac{kL_{BE}}{L_{AB}}\right)}$$

$\Delta L \approx 2d_E$

Tuning thermal expansion coefficient with Copper nanoparticles

Thermal expansion Coefficient
of Cu reinforced PEGDA

$$\alpha_2 \approx \frac{\phi_C K_C \alpha_C + (1-\phi_C) K_1 \alpha_1}{\phi_C K_C + (1-\phi_C) K_1}$$

Volume fraction ϕ

Bulk modulus K

Cu α_C ~2×10^{-5} K^{-1}

PEGDA α_1 ~15.6×10^{-5} K^{-1}

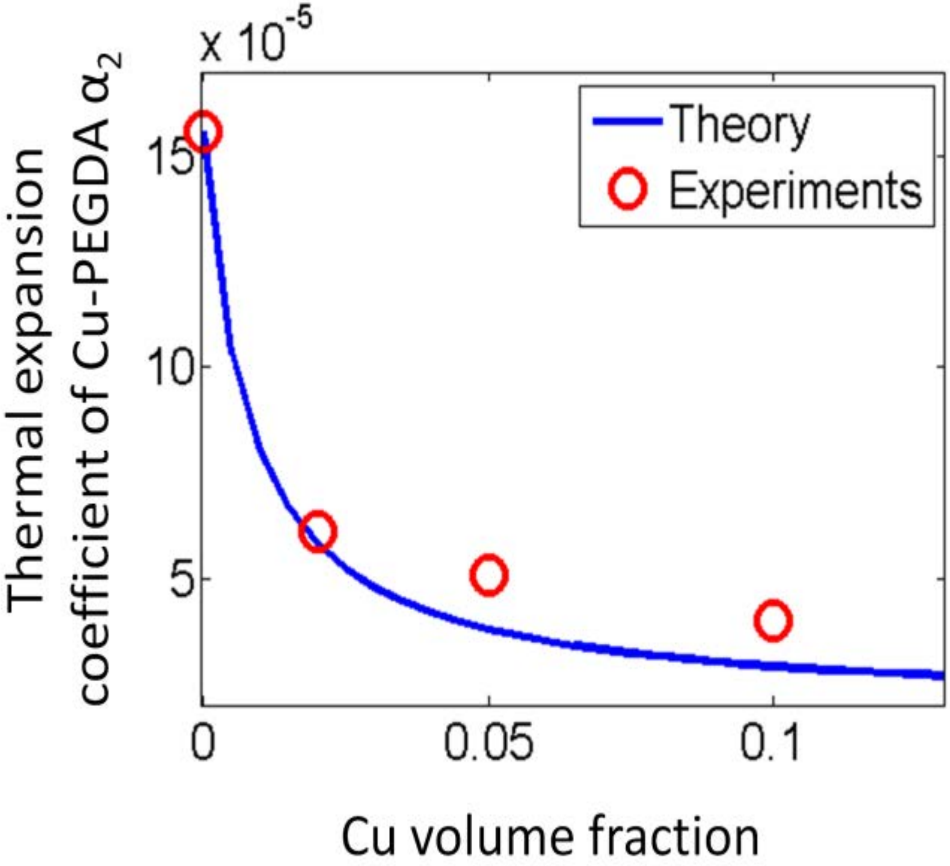

Effective Properties of Composite Materials

Materials / Properties	PEGDA	2Vol%Cu -PEGDA	5Vol%Cu -PEGDA	10Vol%Cu- PEGDA
Young's Modulus $E_x = E_y$ (MPa)	20.3	67.2	90.7	105.5
Young's Modulus E_z (MPa)	23.5	71.1	92.2	112.4
Effective Young's modulus E (MPa)	21.9	69.2	91.5	108.9
Poisson's ratio	~0.4	~0.3	~0.3	~0.3
Thermal expansion coefficient $\alpha_x = \alpha_y (x10^{-6}\ K^{-1})$	153	62.6	51.2	41.4
Thermal expansion coefficient α_z $(x10^{-6}\ K^{-1})$	158.2	59.2	49	38.2
Effective thermal expansion coefficient α $(x10^{-6}\ K^{-1})$	155.6	60.9	50.6	39.8

Deformation Trapping

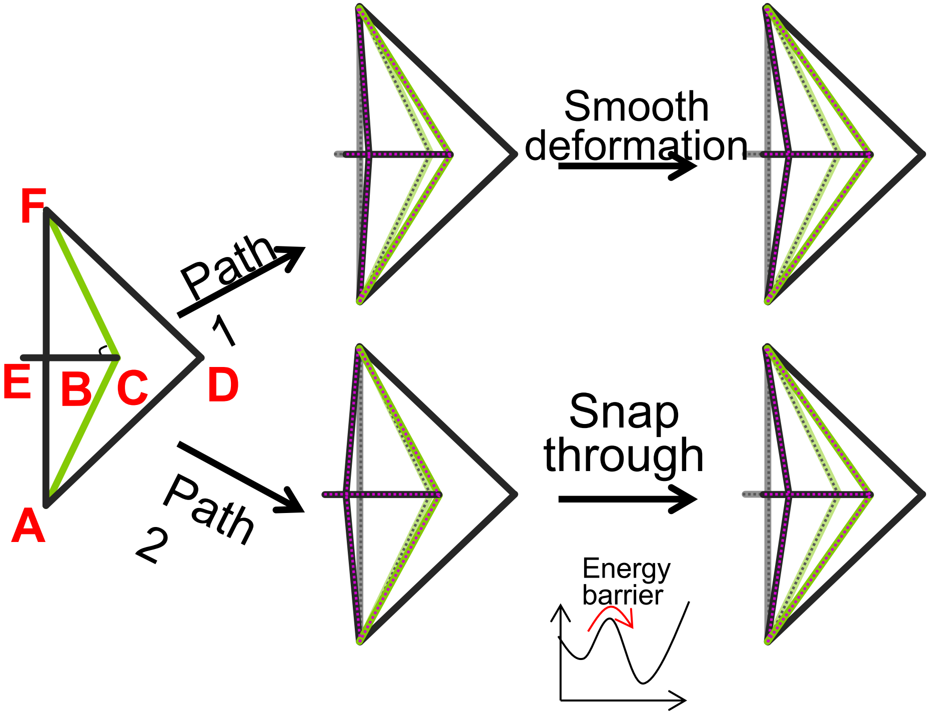

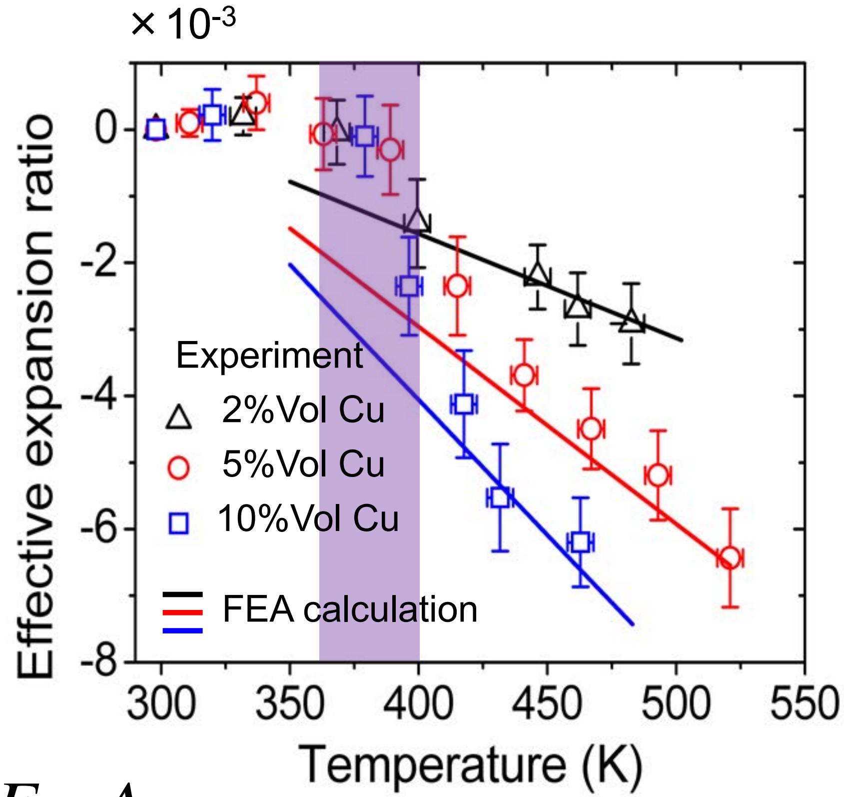

Thermal-induced force within beam AB can be approximated as $\sim \alpha_2 \Delta T E_{AB} A_{AB}$

Critical compressive force for the buckling of beam AB is $\pi^2 E_{AB} I_{AB} / \left(4L_{AB}^2\right)$

Critical temperature $\Delta T_c \sim \dfrac{\pi^2}{3\alpha_2}\left(\dfrac{h_{AB}}{L_{AB}}\right)$ ΔT_c~68.5-102.8 K

Shown in purple shaded area

Tunable CTE Materials:

Preliminary Study by copper solid loading

Tunable CTE from 1.57 × 10^{-5} K^{-1} to 4.06 × 10^{-5} K^{-1}

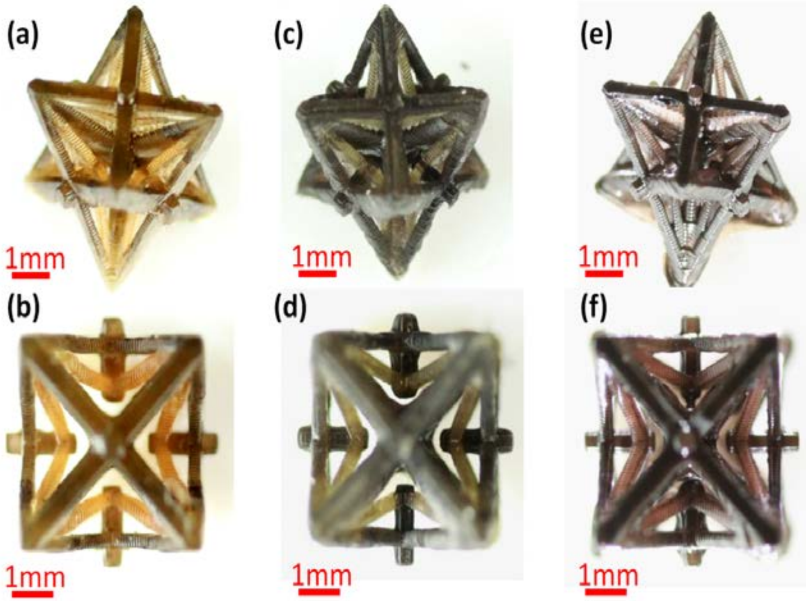

2% vol Cu **5% vol Cu** **10% vol Cu**

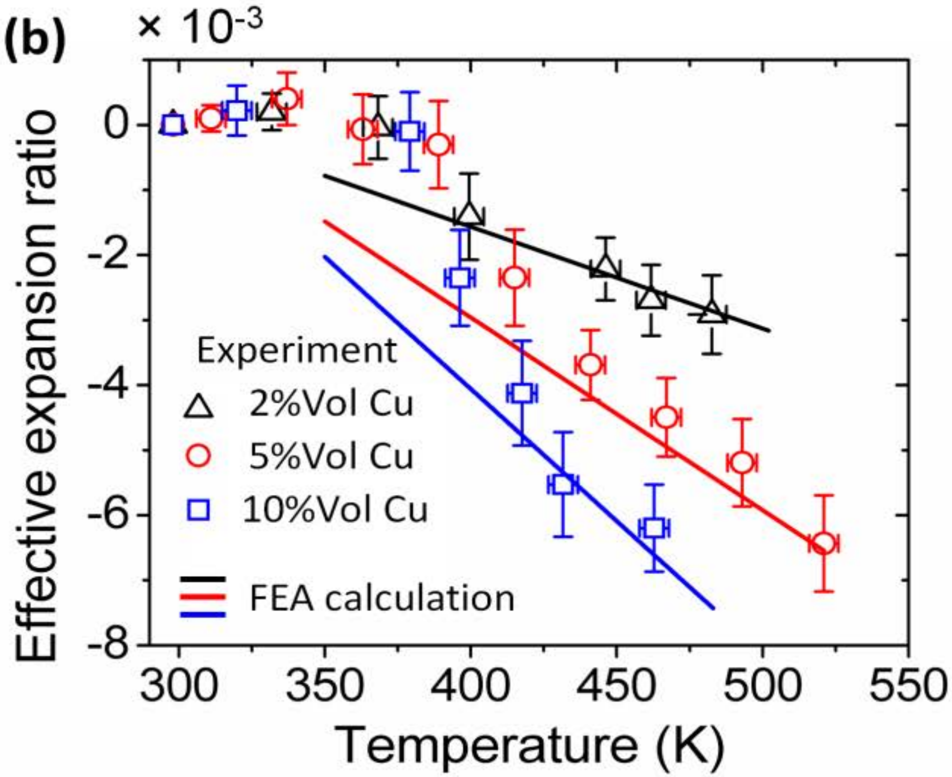

Commercial RF Meta:
E.G. PARC’s “radar digital eye”

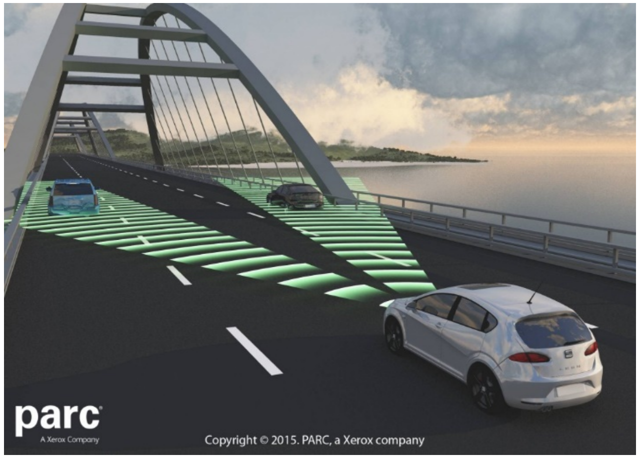

Copyright © 2015. PARC, a Xerox company

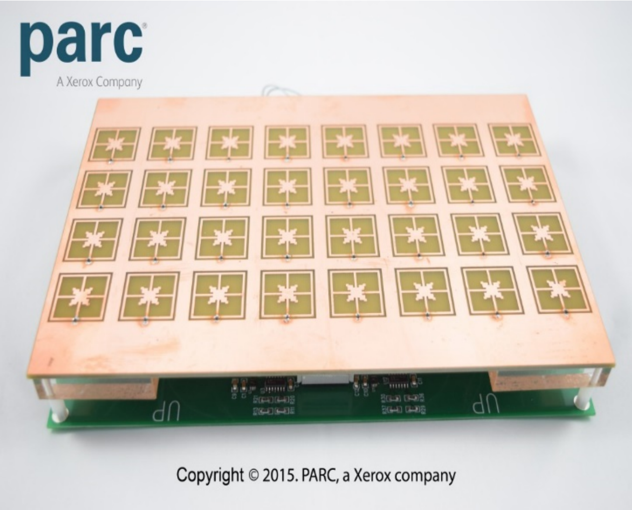

Copyright © 2015. PARC, a Xerox company

- According to PARC, It has a strong enough signal to detect non-metallic objects, and it forms a narrow enough beam to be able to discriminate small objects.
- In real-life, this means that it’s able to discriminate humans in congested environments, e.g., detecting a child running around in a parking lot, or mapping out a cyclist on a curve.
- Current state-of-the-art automotive radars cannot reliably accomplish the same feat, because they rely on digital beam forming (DBF) techniques, which either support high resolution, or high signal-to-noise ratio, but not both.

Examples of Commercial Metamaterials

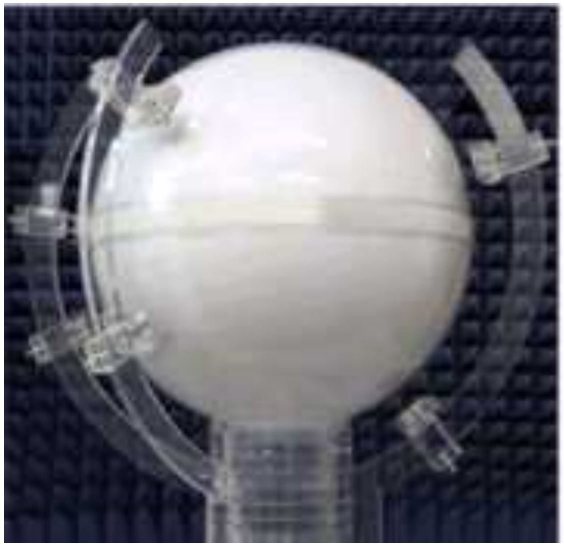
Luneberg lens by LUN'TECH

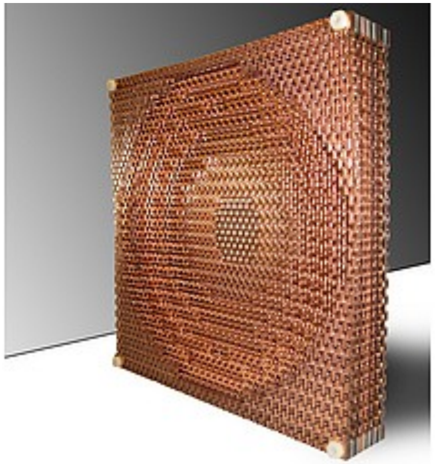
http://news.mit.edu/2012/new-metamaterial-lens-focuses-radio-waves-1114

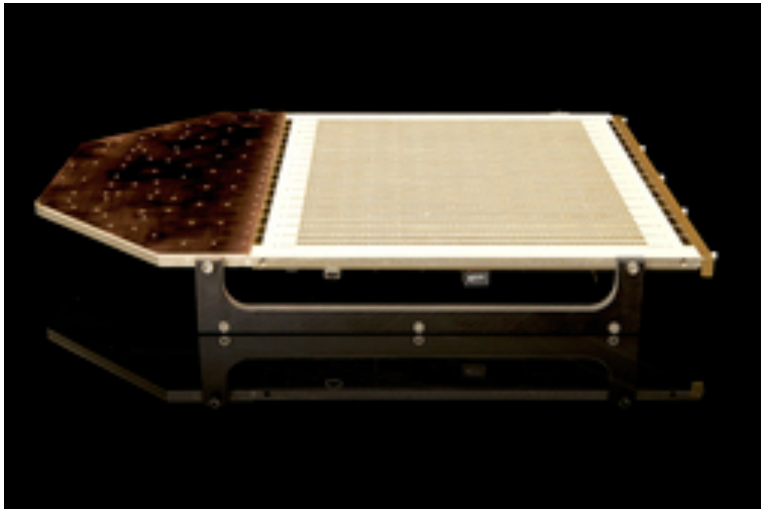
satellite broadband receiver by Kymeta

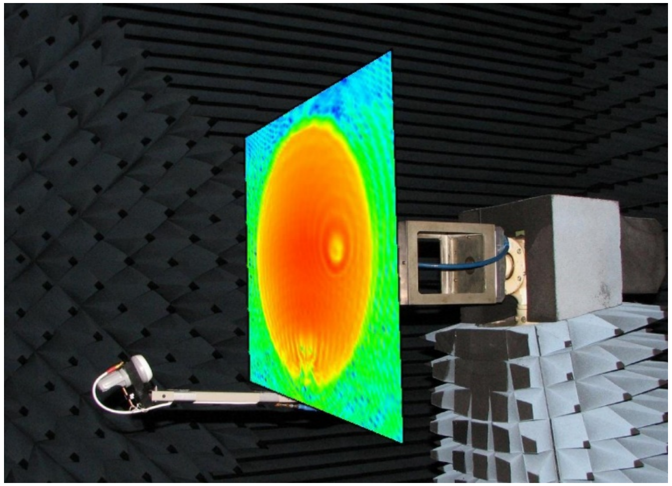
surface conformal antenna

Application Ideas I: Slow Wave Sensor with Amplified Pressure Sensitivity

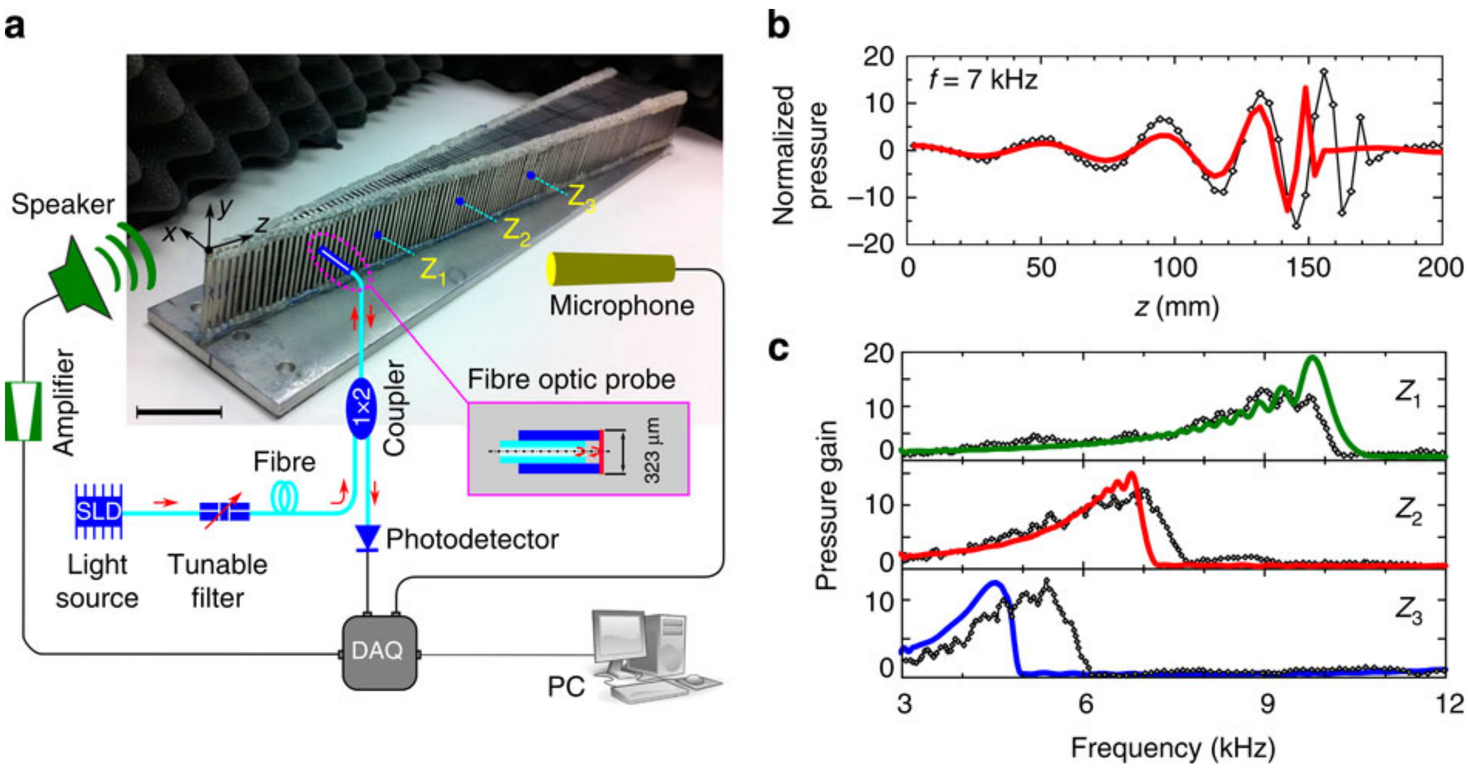

Enhanced acoustic sensing through wave compression and pressure amplification in anisotropic metamaterials
Y Chen, H Liu, M Reilly, H Bae, M Yu
Nature communications 5, 5247, 2014

Application Ideas II:
Compressive Acoustic Sensor

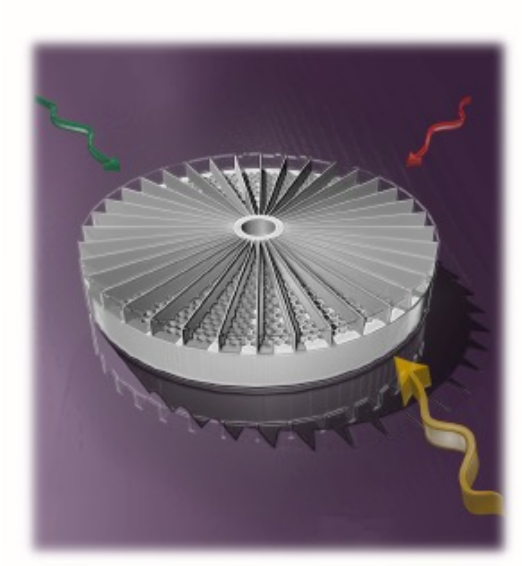

Single-sensor multispeaker listening with acoustic metamaterials
Y Xie, TH Tsai, A Konneker, BI Popa, DJ Brady, SA Cummer
Proceedings of the National Academy of Sciences 112 (34), 10595-10598

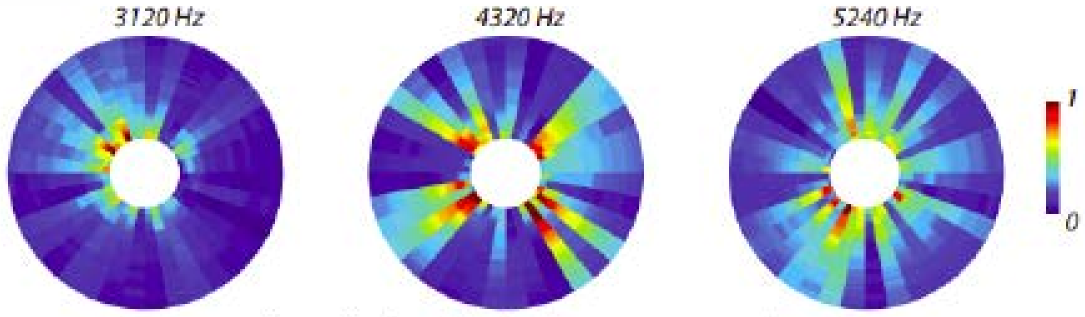

Normalized amplitude of measurement modes

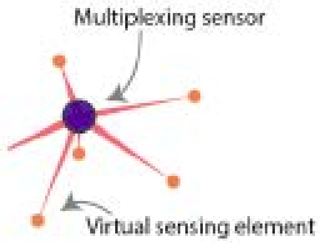

Knowles Electronics, LLC

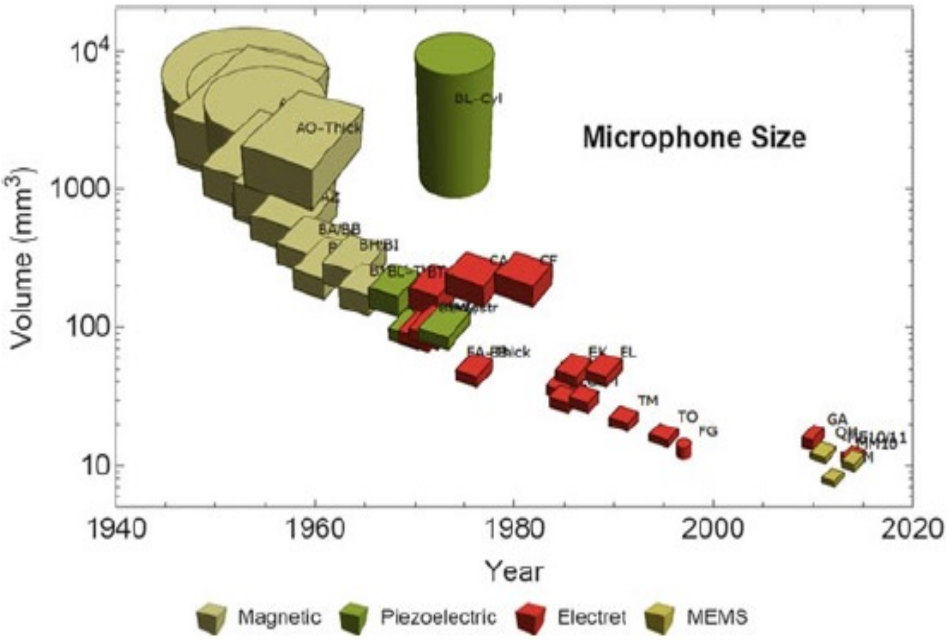

Sphere 48-35 AC Pro

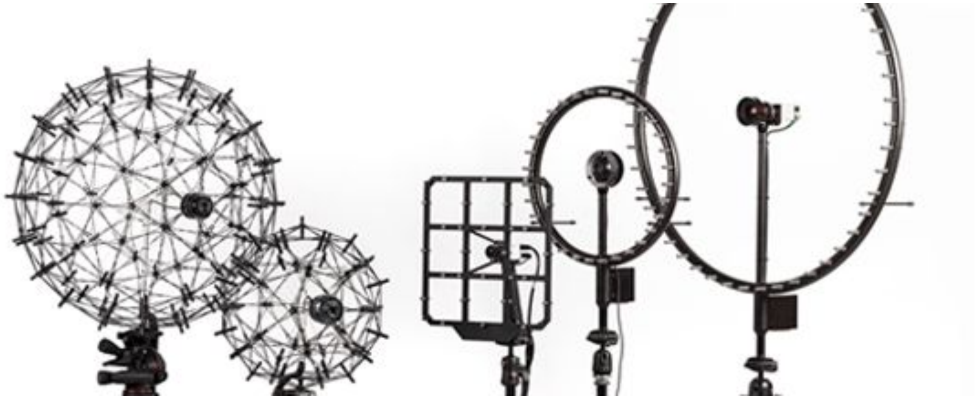

Characteristics
- •48 microphones
- •35 cm diameter
- •carbon fibre structure
- •13-17 dB single map dynamic (CBF)
- •recommended measurement distance: 0.3-5 m
- •recommended mapping frequencies: 400 Hz-15 kHz

Johnson-Champoux-Allard Model

- Replace porous material by equivalent fluid of effective density ($\tilde{\rho}(\omega)$)

$$\tilde{\rho}(\omega) = \rho_0 \alpha_\infty \left[1 + \frac{\sigma\emptyset}{j\omega\rho_0\alpha_\infty} G_J(\omega)\right]$$

- and effective bulk modulus (($\widetilde{K}(\omega)$).

$$\widetilde{K}(\omega) = \frac{\gamma P_0}{\left[\gamma - (\gamma - 1)\left(1 + \frac{8\eta}{j\omega\rho_0 B^2 \Lambda'^2} G_j'(\omega)\right)^{-1}\right]}$$

- Relating to five macroscopic properties:

$\sigma \left(\frac{N.s}{m^4}\right)$; $\emptyset(\%)$; α_∞; $\Lambda(\mu m)$ and $\Lambda'(\mu m)$

Viscous Correlation Factor

$$G_J(\omega) = \sqrt{1 + j\frac{4\omega\eta\rho_0\alpha_\infty^2}{\sigma^2\Lambda^2\emptyset^2}}$$

$$G_j'(\omega) = \sqrt{1 + j\frac{\omega\rho_0 B^2\Lambda'^2}{16\eta}}$$

$$\Lambda = \frac{1}{c}\sqrt{\frac{8\alpha_\infty\eta}{\emptyset\sigma}}$$

Thermal Correlation Factor

$$\Lambda' = \frac{1}{c'}\sqrt{\frac{8\alpha_\infty\eta}{\emptyset\sigma}}$$

Current status in 3D printing

	μSLA	**DIW**	**SLS**	**2PP**	**SPPW**	**VEL**
Resolution	High (~ 1μm)	Low (25~50μm)	Low (50μm)	High (~ 150nm)	Med (~ 5μm)	High (~ 2μm)
Throughput	Low	Med	Low	Very low	High	NA
Scalability	Low	Low	Low	Very low	High	Med
Arbitrary Structuring	Yes	Yes	Yes	Yes	No (lattice)	No (channel)
Material Diversity	Med	High	Med	Low	Low	Med
System Compatibility	High	High	Med	Low	Med	Low
System Complexity	Med	Med	High	High	Low	Low
Printing Unit	Layer	Voxel	Voxel	Voxel	Volume	Volume

3D Microfabrication in Single Snapshot

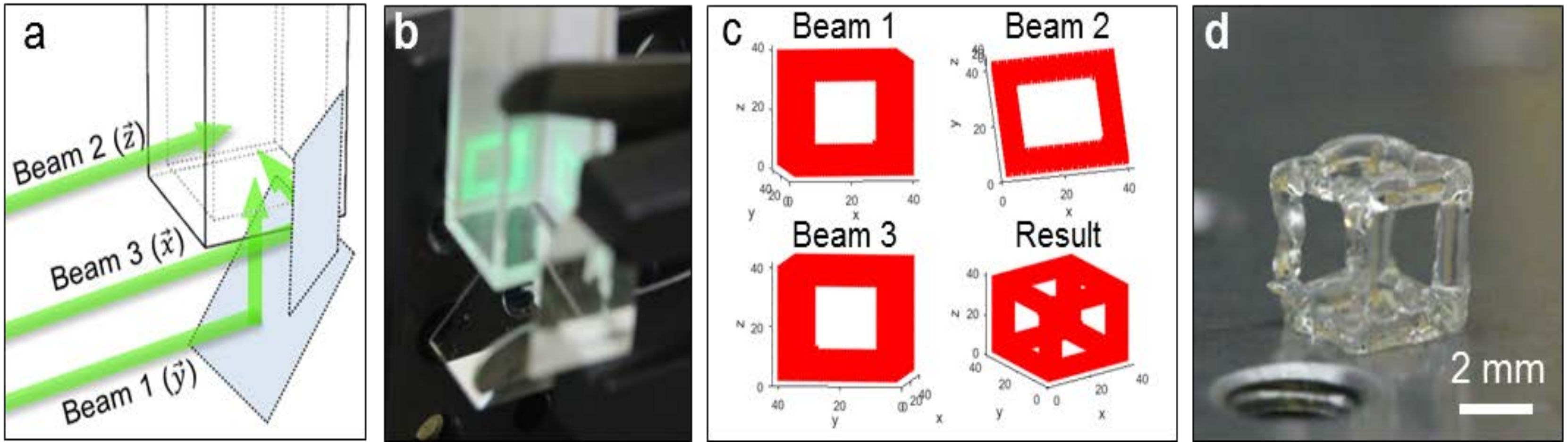

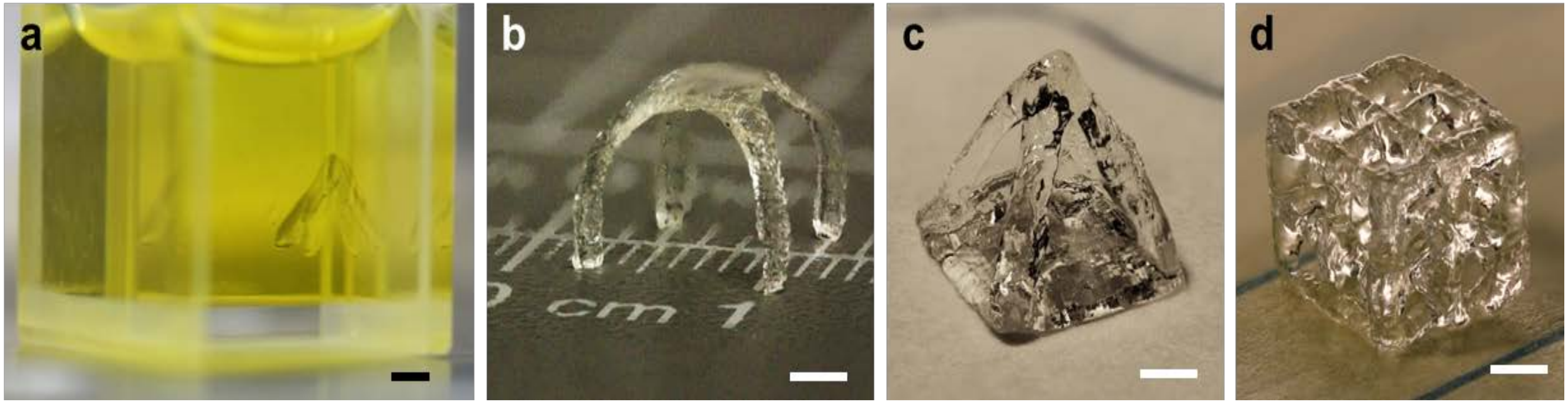

Acoustic Beaming: State Of the Art

Challenges

- Operating at MHz

  ($\lambda<1$ mm)
- Difficult to Miniaturize: diffraction from finite aperture
- Multi-transducer requirement and high cost

NDT:
1M-10MHz
(from GE Panametrics)

ITC - 3003D

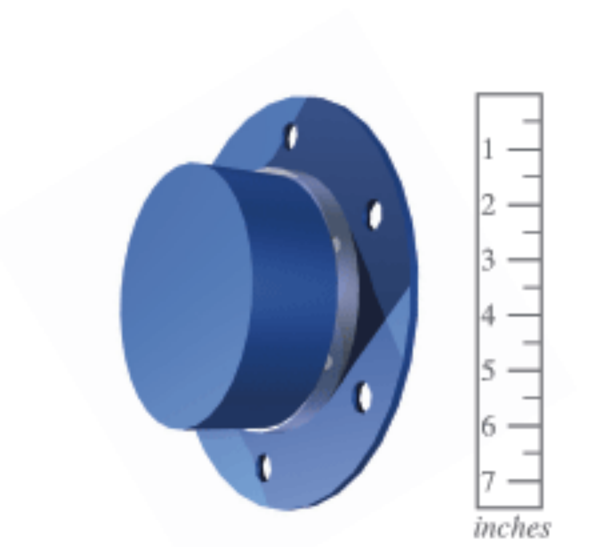

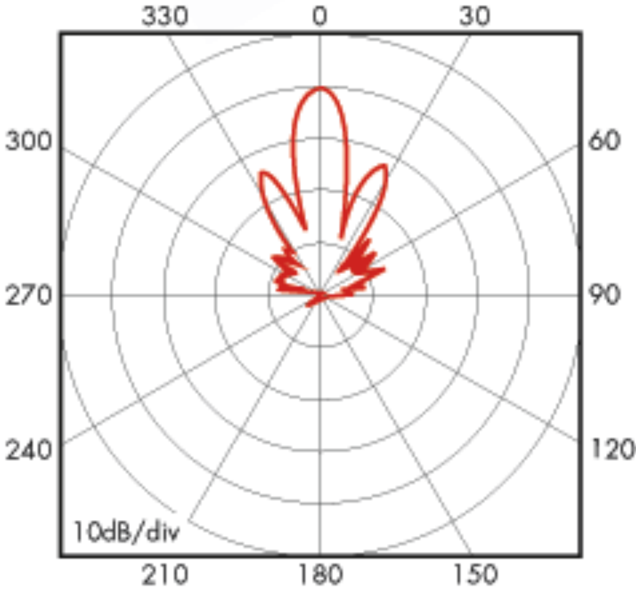

Directivity Pattern at 120.0 kHz

Resonance Frequency	118	kHz
Depth	Unlimited	-
Envelope Dimensions	2.25D x 7.5H	inches
TVR at fr	160	db/µPa/V@1m
Beam Width	10	deg -3dB at fr
Beam Type	Conical	-
Input Power	1000	watts